Bis- and Tris-DNA Intercalating Porphyrins Designed to Target the Major Groove: Synthesis of Acridylbis-arginyl-porphyrins, Molecular Modelling of Their DNA Complexes, and Experimental Tests

Samia Far,[a] Alain Kossanyi,[a] Catherine Verchère-Béaur,[a] Nohad Gresh,[b] Eliane Taillandier,[c] and Martine Perrée-Fauvet*[a]

Keywords: Cationic porphyrins / Molecular modelling / DNA intercalation / DNA recognition / Topoisomerase I

In order to increase the DNA binding affinity of a bis-arginyl-porphyrin which has been previously shown to bind preferentially in the major groove of the d(GGCGCC)$_2$ sequence (Mohammadi et al., *Biochemistry* **1998**, *37*, 9165), we have synthesized bis- and tris-intercalating derivatives in which one or both arginyl arms are connected through a flexible chain to an acridine ring. We report here the synthesis of these two molecules along with the molecular modelling of their complexes with a GC-rich oligonucleotide encompassing the central d(GGCGCC)$_2$ hexamer. The modelling computations showed that when the porphyrin was intercalated into the central d(CpG)$_2$ site with both arginyl side-chains bonded to the guanines flanking the intercalation site, the acridine ring(s) could intercalate immediately upstream from the central hexamer, but at the cost of substantial DNA conformational energy. A significant preference for major-groove binding over minor-groove binding was found. The results of circular dichroism studies and topoisomerase I-unwinding experiments supported the bis- and tris-intercalation of these derivatives. The bis-acridyl derivative provided, as expected, greater stabilization against thermal denaturation than the mono-acridyl and the parent bis-arginyl-porphyrin compounds. Based on the modelling results, the structures of derivatives can be tailored to facilitate tris-intercalation in rigid GC-rich sequences, and thereby enhance the selective targeting of GC base pairs by the arginyl side-chains, by lengthening the porphyrin-acridine connectors.

Introduction

Most DNA sequence-specific drugs target the minor groove, as is the case for nonintercalating groove binders[1] and the majority of intercalators[2] and oligopeptide-intercalator conjugates.[3] Major-groove recognition can be achieved by extended oligomeric motifs such as synthetic antigene oligonucleotides[4] and their intercalator conjugates,[5] peptide nucleic acids,[6] oligopeptides stitched together by disulfide bonds,[7] and peptide complexes of iron[8] as well as of rhodium or ruthenium metallointercalators,[9] but by only very few smaller-sized ligands.[10–14]

On the basis of theoretical computations, we previously synthesized a bis-arginyl derivative of a tricationic porphyrin (Figure 1, BAP) which was designed to bind specifically to the palindromic sequence d(GGCGCC)$_2$.[15] The DNA binding of the parent compound, *meso*-tetrakis(*N*-methyl-4-pyridiniumyl)porphyrin or H_2TMPyP-4, has been widely studied,[16] and its ability to intercalate into CpG or GpC steps or to bind in a groove at A-T rich sequences has been shown. This porphyrin also has DNA-photosensitizing[17] and antitumour properties.[18] BAP modelling studies have shown that the two Arg arms of the bis-arginyl derivative bind preferentially to the major groove of DNA, the best-bound sequence being the palindromic sequence d(GGCGCC)$_2$.[19] In the energy-minimized structure, the porphyrin ring was intercalated into the central d(CpG)$_2$ sequence so that each Arg arm was bound to a distinct DNA strand and the guanidinium groups were hydrogen-bonded to two O^6/N^7 atoms of the two successive guanines upstream from the intercalation site. Simultaneous interactions of an Arg side-chain with two successive G bases on the same strand have been observed in an X-ray diffraction

[a] Laboratoire de Chimie Bioorganique et Bioinorganique
Institut de Chimie Moléculaire et des Matériaux d'Orsay, CNRS UMR 8124, Bât. 420 Université Paris-Sud, 91405 Orsay Cedex, France
Fax: (internat.) +33-169157281
E-mail: mperreef@icmo.u-psud.fr
[b] Laboratoire de Pharmacochimie Moléculaire et Cellulaire, CNRS FRE 2718, UFR Biomédicale, Université René-Descartes (Paris V)
45, rue des Saints-Pères, 75006 Paris, France
[c] Laboratoire de Spectroscopie Biomoléculaire, UFR de Santé, Médecine et Biologie Humaine, Université Paris-Nord
74 rue Marcel Cachin, 93017 Bobigny, France

Supporting information for this article is available on the WWW under http://www.eurjoc.org or from the author.

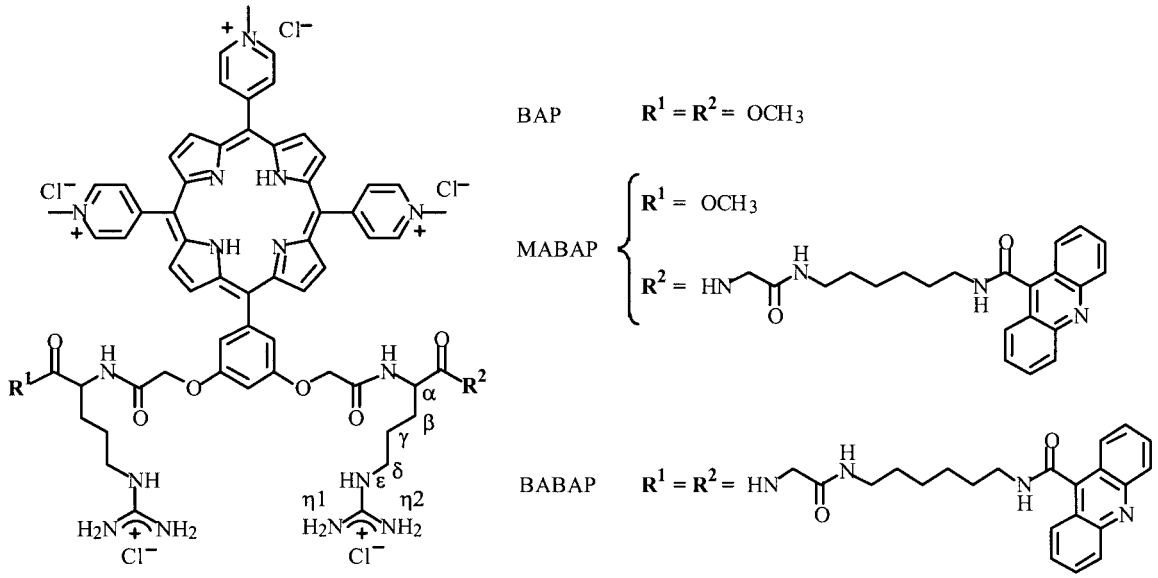

Figure 1. Molecular structure of BAP, MABAP and BABAP compounds

study of the complex of the DNA-binding domain of yeast RAP1 with telomeric DNA.[20]

Spectroscopic IR studies carried out on BAP-oligonucleotide complexes have confirmed that the Arg arms are located in the major groove of G-C rich complexes and thermal denaturation studies showed that the best relative stabilization occurs on d(GGCGCC)$_2$-encompassing sequences.[21]

The GGCGCC sequence occurs frequently in oncogenes[22] and is also found in the Primer Binding Site (PBS) of the Long Terminal Repeat (LTR) of the HIV retrovirus.[23] Thus, ligands that recognize this sequence with enhanced affinity and selectivity could have promising antitumour or antiviral properties. Towards this aim, we have extended the structure of BAP by linking to one, or both, Arg arms a second, or third, intercalator, of acridine type, through an additional Gly residue and a polymethylenic chain. Considerable enhancements of DNA-binding affinities have previously been demonstrated upon passing from mono- to bis- and tris-intercalating derivatives.[24] The syntheses of porphyrin-mono- and bis-acridine conjugates have recently been reported[25] and these molecules are endowed with significant nuclease[25a,25c,25d] and cytotoxic[25b] activities. Although acridines have low sequence selectivities, except possibly in favour of intercalation at pyr-pur steps over pur-pyr steps, the purpose of their inclusion is essentially that of reinforcing the DNA-binding affinities of porphyrin-peptide conjugates.

Here we report the molecular modelling of the complexes of two acridylbis-arginyl-porphyrins with a double-stranded sequence d(CTGTTCGGGCGCCCGAACAG)$_2$ encompassing an undecanucleotide fragment of the HIV-1 PBS.[23] This constitutes a prerequisite to their chemical synthesis, which is subsequently reported together with DNA-interaction experiments.

Results and Discussion

Molecular Modelling of DNA Complexes of Acridylbis-arginyl-porphyrins

Oligonucleotide Sequence

We have modelled the interaction of acridyl derivatives of bis-arginyl-porphyrin (BAP) with the palindromic sequence d(CTGTTC GGGC GCCC GAACAG)$_2$ (Figure 2). The intercalation sites are d(C^6-G^7)·d(C$^{14'}$-G$^{15'}$) and d(C^{14}-G^{15})·d(C$^{6'}$-G$^{7'}$) for the acridine rings and d(C^{10}-G^{11})·d(C$^{10'}$-G$^{11'}$) for the porphyrin ring. We present below the most favourable binding modes of two selected BAP derivatives, denoted as mono-acridyl-bis-arginyl-porphyrin (MABAP) and bis-acridyl-bis-arginyl-porphyrin (BABAP).[26] Their structures are given in Figure 1. In these derivatives, the acridine ring is bound to the arginine through a glycine and a hexamethylene diamine linker.

Mono-acridyl-bis-arginyl-porphyrin (MABAP)

Three binding modes, each with the phenyl group (bearing the arginyl arms) located in the major groove, were compared: they have three, two, and one *N*-methylpyridinium rings in the minor groove and were denoted as A, C, and B, respectively, in our preceding papers on the mono-intercalating parent compound BAP.[19,21] For each of these modes, the acridyl ring can intercalate at the d(C^{6}pG^7)·d(C$^{14'}$pG$^{15'}$) site from either the major-groove side (denoted as 'I', internal mode), or from the minor-groove side (denoted as 'E', external mode). In the latter case, the aliphatic acridine connector winds around the sugar-phosphate backbone.

The two most favourable modes of binding to the PBS-encompassing sequence are modes A-I and C-I (Table 1).

C^{1} T^{2} G^{3} T^{4} T^{5} C^{6} G^{7} G^{8} G^{9} C^{10} G^{11} C^{12} C^{13} C^{14} G^{15} A^{16} A^{17} C^{18} A^{19} G^{20}
$G^{20'}$ $A^{19'}$ $C^{18'}$ $A^{17'}$ $A^{16'}$ $G^{15'}$ $C^{14'}$ $C^{13'}$ $C^{12'}$ $G^{11'}$ $C^{10'}$ $G^{9'}$ $G^{8'}$ $G^{7'}$ $C^{6'}$ $T^{5'}$ $T^{4'}$ $G^{3'}$ $T^{2'}$ $C^{1'}$

Figure 2. Base numbering of the double-stranded d(CTGTTC GGGC GCCC GAACAG)$_2$

Table 1. Binding energies (kcal·mol^{-1}) of the intercalation of MABAP in the sequence d(CTGTTC GGGC GCCC GAACAG)$_2$; the arginine side-chains interact in the major groove

Intercalation mode of the porphyrin	A	B		C	
Intercalation mode of the acridine	I	I	E	I	E
E_{inter}	−325.0	−330.8	−320.2	−350.8	−314.0
ΔE_{DNA}	142.8	145.8	134.2	144.4	130.2
ΔE_{lig}	35.4	60.1	71.3	57.5	80.0
$E = E_{inter} + \Delta E_{DNA} + \Delta E_{lig}$	−146.8	−124.9	−114.7	−148.9	−103.8

They are represented in Figure 3 (a) and (b) respectively. In mode A-I, the Arg side-chain, which precedes the acridine, interacts with O^6/N^7 of guanines G^7, G^8 and G^9 upstream from the intercalation site. The side-chain of the other arginine interacts with N_7 of $G^{8'}$ and O^6 of $G^{9'}$ upstream from the intercalation site, and with O^6/N^7 of G^{11} of the intercalation site. In binding mode C-I, the acridine-connected arginine binds to O^6 of $G^7$and G^8 and to N^7 of G^9. The other arginine binds to $G^{7'}$, $G^{8'}$ and to $G^{9'}$ as well as to O^6 of G^{11} of the intercalation site.

Bis-acridyl-bis-arginyl-porphyrin (BABAP)

As in the case of MABAP, the three modes A, B, and C were considered. Mixed modes of the type IE, in which one acridine intercalates from the minor-groove side and the other from the major-groove side, were also considered. The most favourable complexes of BABAP with the PBS-encompassing sequence in modes A−C are shown in Figure 4 (a−c). The stabilities of the three complexes are ranked in the order A-II > B-EE > C-II (Table 2).

The most favourable A binding mode is II, in which both acridines intercalate from the major groove side. The side-chain of one Arg interacts with the three successive guanines G^7, G^8, G^9 upstream from the intercalation site. The side-chain of the other Arg similarly spans $G^{7'}$, $G^{8'}$, and $G^{9'}$ on the other strand.

The most favourable B binding mode is EE, favoured over II because the porphyrin ring, which protrudes more in the major groove, causes the peptide backbone to be

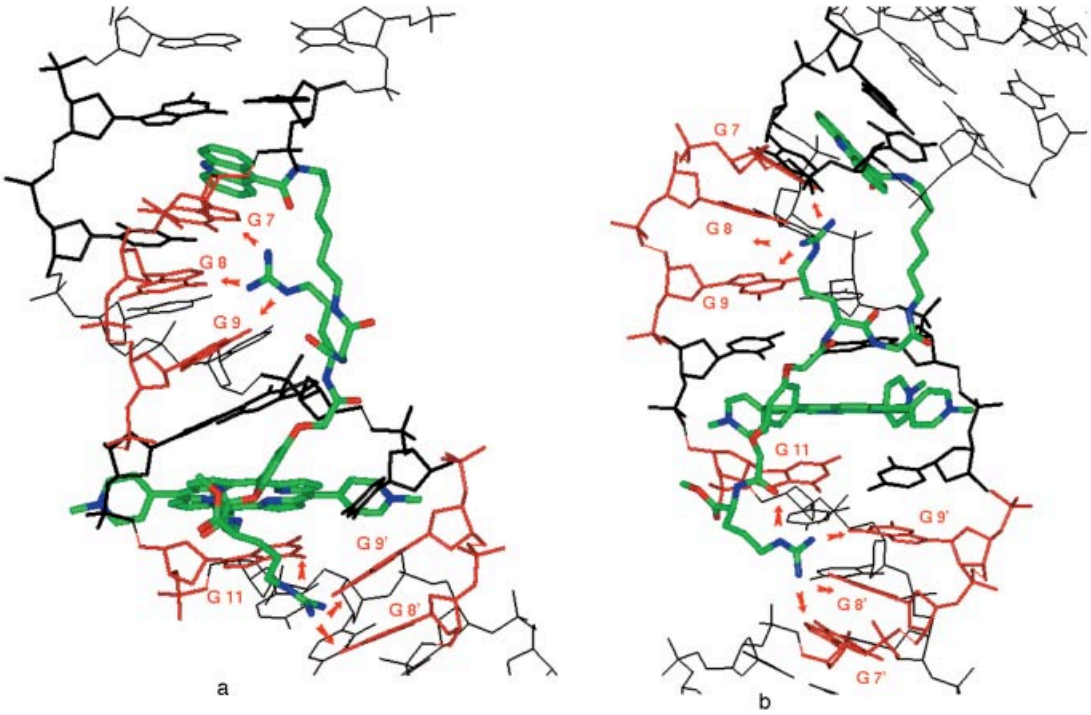

Figure 3. Molecular modelling of two intercalated complexes of MABAP in the sequence d(CTGTTC GGGC GCCC GAACAG)$_2$; the arginine side-chains interact in the major groove: (a) mode A-I; (b) mode C-I (hydrogens are omitted for clarity)

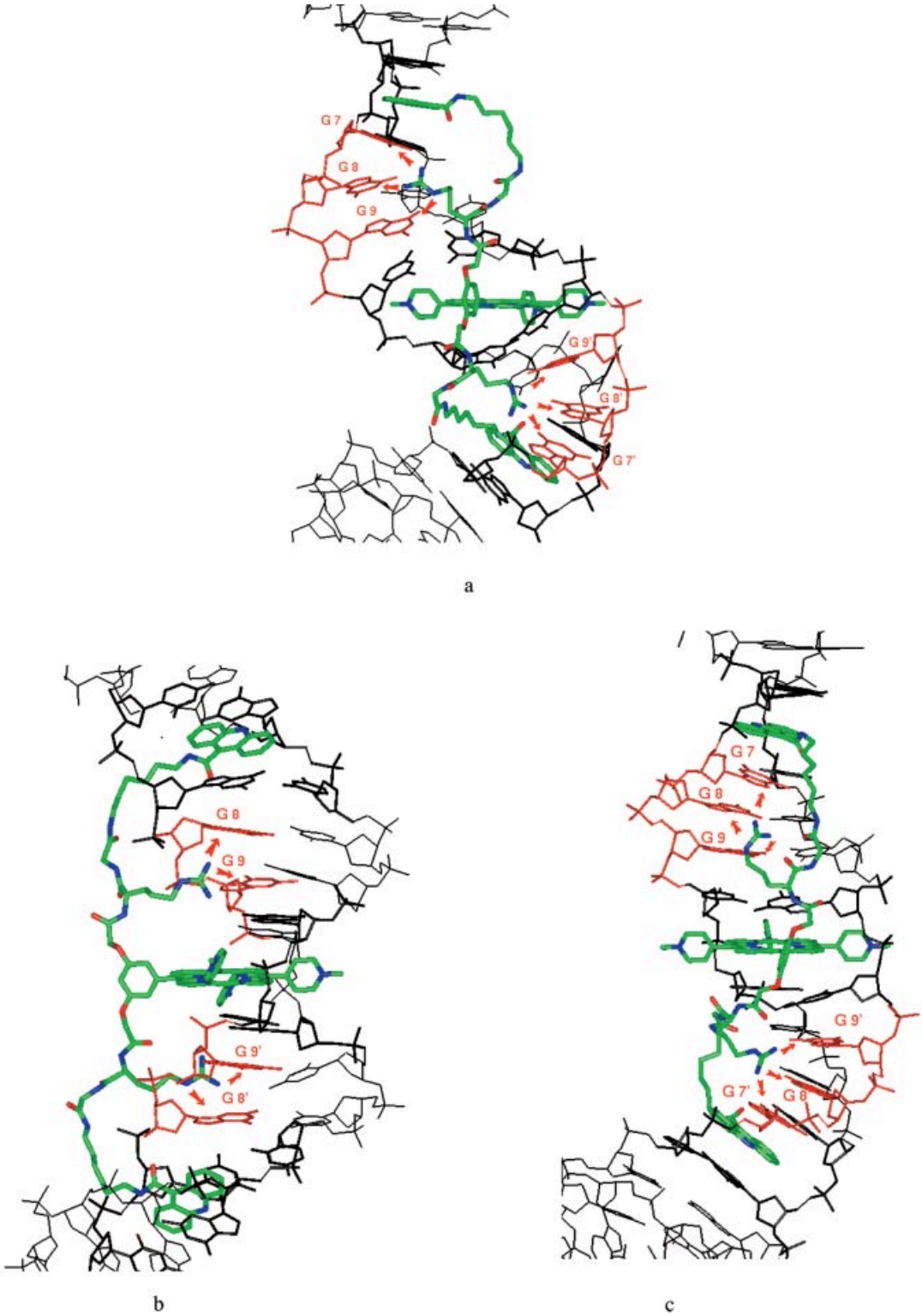

Figure 4. Molecular modelling of three intercalated complexes of BABAP in the sequence d(CTGTTC GGGC GCCC GAACAG)$_2$; the arginine side-chains interact in the major groove: (a) mode A-II; (b) mode B-EE; (c) mode C-II (hydrogens are omitted for clarity)

shifted more towards the periphery thus facilitating winding of the aliphatic acridine connector around the DNA backbone. One Arg side-chain binds to G^8 and G^9 on the unprimed strand, and similarly the other Arg binds to $G^{8'}$ and $G^{9'}$ on the primed strand. They also interact respectively with $G^{11'}$ and G^{11} of the intercalation site.

Table 2. Binding Energies (kcal·mol^{-1}) of the intercalation of BABAP in the sequence d(CTGTTC GGGC GCCC GAACAG)$_2$. The arginine side-chains interact in the major groove

Intercalation mode of the porphyrin	A		B		C	
Intercalation mode of the acridine	II	II	EE	IE	II	IE
E_{inter}	−432.5	−332.5	−399.7	−410.5	−375.1	−405.2
ΔE_{DNA}	148.0	138.9	128.6	154.0	157.9	158.9
ΔE_{lig}	136.0	103.0	137.1	129.3	89.9	132.0
$E = E_{\text{inter}} + \Delta E_{\text{DNA}} + \Delta E_{\text{lig}}$	−148.5	−90.6	−134.0	−127.2	−127.3	−114.3

Similar to mode A, the most favourable C binding mode is II. On the unprimed strand, one Arg interacts with G^7, G^8 and G^9 and on the primed strand, the other Arg interacts with G$^{7'}$, G$^{8'}$ and G$^{9'}$.

For both MABAP and BABAP, the amount of DNA conformational distortion energy, ΔE_{DNA}, in the range 129−159 kcal·mol^{-1}, is considerable. For comparison, it is recalled that in the complex of a DNA double-stranded dodecamer with the mono-intercalating porphyrin-netropsin derivative,[27] also studied by the JUMNA procedure, ΔE_{DNA} had values in the range 45−70 kcal·mol^{-1}, yet the DNA was shorter than in the present study and had undergone less severe distortions. Such large values may reflect the sensitivity of the JUMNA potential to DNA distortions. Note that in the present case it is the E_{inter} term that determines the most stable binding complexes for MABAP (C-I) and BABAP (A-II).

Taking into account the fact that a more attractive electrostatic potential is exerted on positive charges in the minor groove by A-T-rich sequences than by G-C-rich ones,[28] we have also computed the energy balances for the intercalated complexes of BABAP in the sequence d(CTGTAT ATAC GTAT ATACAG)$_2$. The central hexameric sequence in this case is d(TACGTA)$_2$ instead of d(GGCGCC)$_2$, and the phenyl group (bearing the arginyl arms) is therefore located in the minor groove of the oligonucleotide. The energy balance in the best minor-groove binding mode (A-II) was found to be less favourable than that in the best major groove binding mode of BABAP. Such a difference is somewhat larger than that previously reported for the parent mono-intercalating compound BAP.[19] Notwithstanding the quantitative limitations inherent to the simplified approach followed in this study, with only implicit modelling of environmental effects, this could imply that enhancement of the major- versus minor-groove preference would result on passing from mono- to tris-intercalation, provided the targeting peptide side-chains are properly oriented.

The most favourable major groove BABAP complex, A-II, has a significantly lower E_{inter} value than those found for the most stable MABAP complexes A-I and C-I. This is compensated, however, by much larger ligand conformation energy rearrangements, ΔE_{lig}, for BABAP than for MABAP. As a result, the energy balances, which consist of small differences between large and opposing contributions, are virtually identical for both compounds, while the experimental data suggest that BABAP has a stronger affinity than MABAP for DNA. Further refinements of the energy balances could include an explicit, rather than implicit, inclusion of solvation effects using a Continuum reaction field procedure in the JUMNA procedure (Zakrzeswka et al., work in progress).

Finally, it was important to evaluate to what extent the two predominant structural features shown by energy-minimization of the BABAP-DNA complex would be maintained after molecular dynamics in a water bath. These two features are tris-intercalation and the onset of H-bonds between the Arg arms and the guanine bases. We wished to avoid the uncertainties due to the number and distribution of the counterions and prevent excessive distortions of the DNA backbone which could occur if environmental effects are not fully accounted for. Thus, for the present purpose, and because of the *qualitative* nature of the present evaluation, we have used screened phosphate charges of −0.5 (as in JUMNA), and the hydrogen bonds of the base pairs (bp) were enforced with harmonic restraints. This evaluation was limited to the best binding complex A-II. Two separate MD simulations were performed in a bath of 3744 water molecules with periodic boundary conditions. The first was with rigid DNA, and the second with one DNA strand relaxed (as in our former MD study on BAP[19]). The lowest frames from these simulations of 50 ps duration are given in the Supporting Information (see S1-S2). Tris-intercalation is preserved in both cases. While for the first dynamics simulation, the Arg side-chain on the primed strand maintains its H-bonds with all three G bases, G7′-G9′, the Arg on the unprimed strand retains its H-bonds with only G8 and G9. In the second simulation, the Arg side-chain on the primed strand is held in place by ionic H-bonds with the phosphate groups on the 3′- and 5′-sites of guanine G8′ and by hydrogen bonds with guanines G7′ and G9′. It binds to G8′ through water molecules. However the Arg on the unprimed strand loses its H-bonds with the G bases, and interacts with the water. This indicates that the receptor competes with the solvent in its interactions with a ligand's functional group.[29] However, longer simulation times and averaging are needed to better quantify such competition. It could also be very important in the future to evaluate how such competition is reflected by other molecular mechanics potentials that explicitly include polarization and cooperative effects and the energy balance for direct versus through-water binding of a cationic entity to an electron-rich ligand.[30]

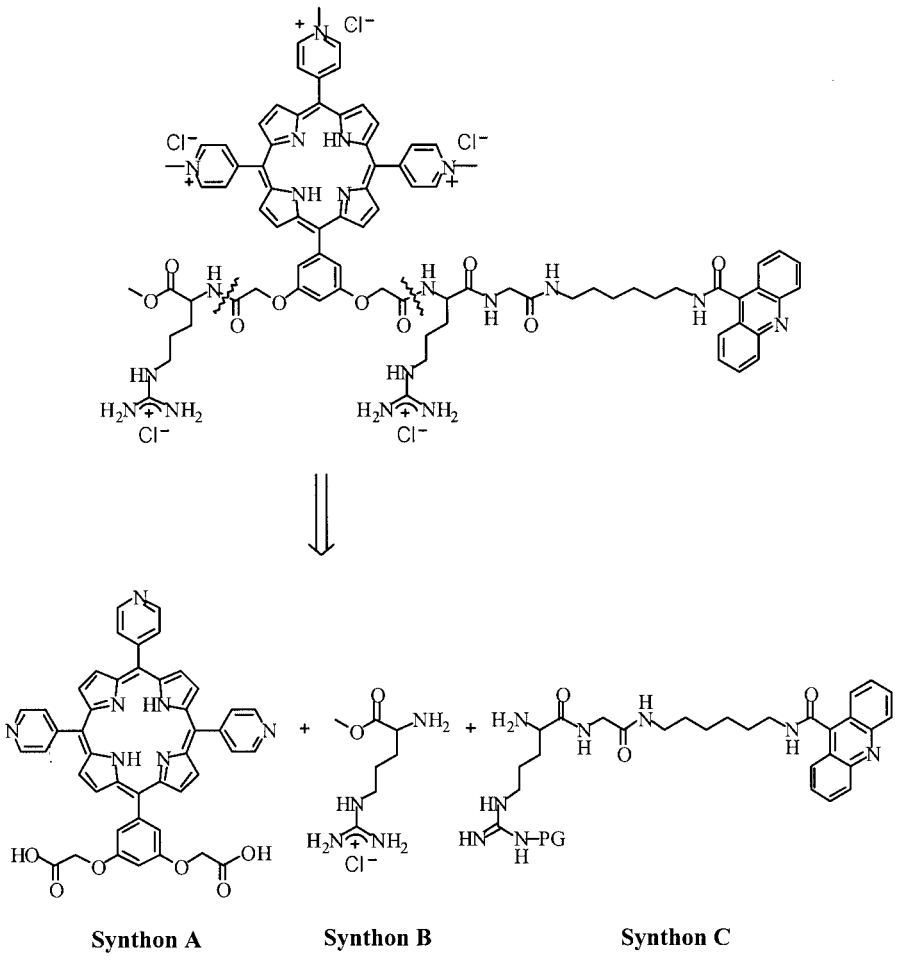

Scheme 1. Retrosynthetic scheme for MABAP synthesis (PG = Protective Group)

Synthesis of the Two Acridylbis-arginyl-porphyrins MABAP and BABAP

The strategy used for synthesizing MABAP is given in the retrosynthetic Scheme 1. It implies the preliminary synthesis of the porphyrinic synthon **A** and the acridyl synthon **C**. BABAP synthesis results from the coupling of synthons **A** and **C**, and BAP was earlier obtained by the coupling of synthons **A** and **B**.[15]

The synthesis of the porphyrin diacid **A** has been described previously.[15] The amino function of the arginine (synthons **B** and **C**) will be used as the anchoring point on the porphyrin **A**. Synthon **B** is a commercial L-arginine methyl ester and synthon **C** consists of a guanidinium-protected arginine connected to an acridine moiety through a glycine and a hexamethylenic chain. The last steps of the synthesis involve the removal of the protective group of guanidinium and methylation of the pyridyl rings of the porphyrin.

Synthesis of Synthon C

The synthon **C** was prepared according to Scheme 2 using a series of peptidic couplings involving four reagents: 9-acridinecarboxylic acid, hexamethylene diamine, glycine and arginine. This requires the preliminary protection of the functional groups carried by reagents that are likely to react during the coupling. The acridine derivative **5**, which was obtained in an overall yield of 60%, was coupled to an arginine protected both on its amine function, to avoid secondary coupling reactions, and on its guanidinium group. The protection of the latter yields arginine derivatives that are easier to purify than their salt form and this protection was retained until the ultimate stage of the synthesis. We chose to protect the guanidinium with the 2,2,4,6,7-pentamethyldihydrobenzofuran-5-sulfonyl (Pbf) protective group, as it is easily cleaved by trifluoroacetic acid,[31] while the arginine amine function was protected by the 9-fluorenylmethoxycarbonyl (Fmoc) group, one of the very rare amine protective groups to be cleaved by bases.[32] The eventual deprotection of the Fmoc group by the amine function of **5** (and to a lesser extent by the base used for the coupling) was reduced if the DMF solution of **5** was diluted and added slowly to an ice-cooled solution of the activated ester of (Fmoc)-Arg(Pbf).[33] Cleavage of the Fmoc group by 1,8-diazabicyclo[5.4.0]undec-7-ene (DBU) gave the synthon **C** which was obtained with an overall yield of 30%.

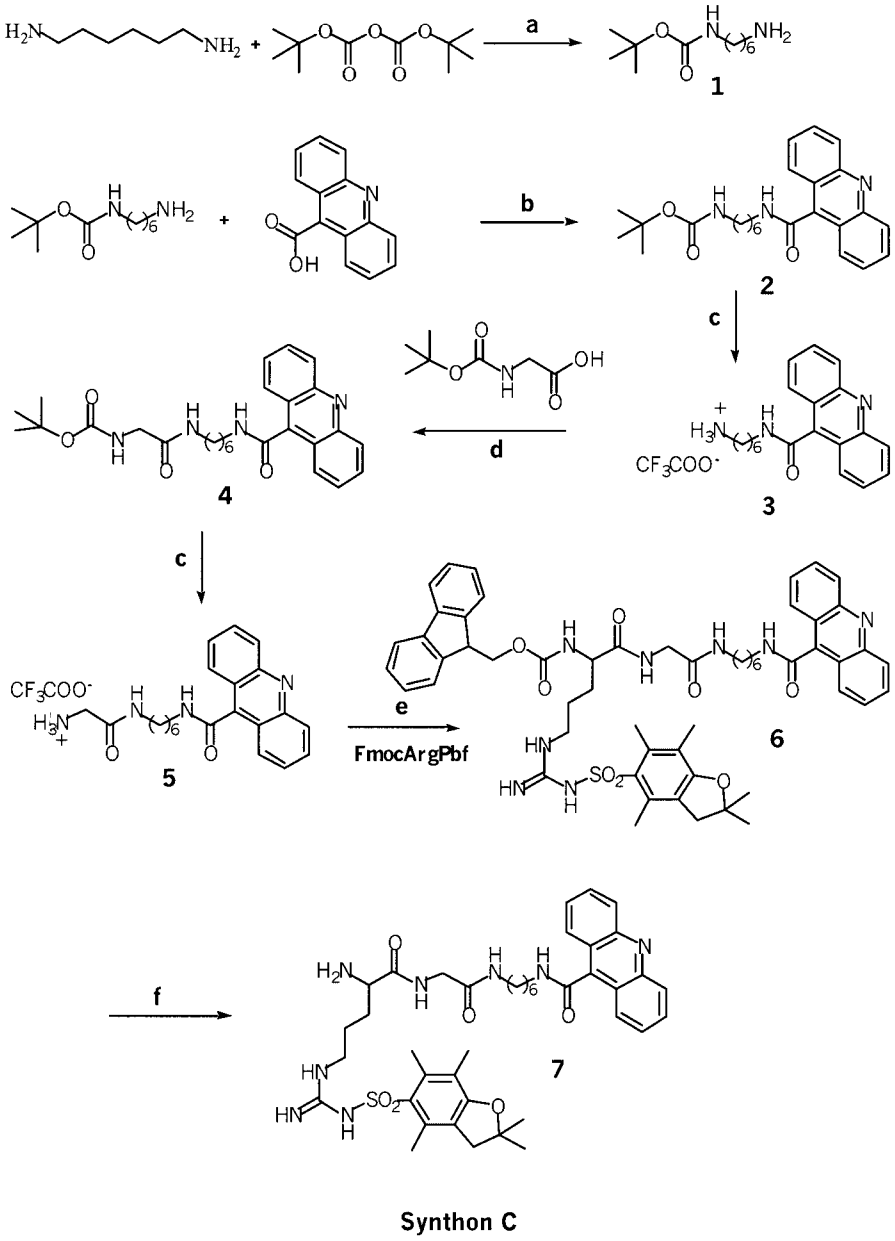

Scheme 2. Synthesis of synthon **C**: (a) dioxane, room temp., 72 h; (b) BOP (1.1 equiv.), DIEA (1.2 equiv.), DMF, room temp., Ar, 24 h; (c) CH_2Cl_2/TFA (v/v), room temp. 1 h; (d) PyBOP (1.2 equiv.), DIEA (5 equiv./**3** +1.2 equiv./Gly), DMF, room temp., Ar, 48 h; (e) BOP (1.2 equiv.), DIEA (5 equiv./**5** +1.2 equiv./Arg), DMF, room temp., Ar, 24 h; (f) DBU, THF, room temp., 15 min

Synthesis of MABAP

MABAP was synthesised by the coupling of the porphyrin diacid (synthon **A**) with synthons **B** and **C**, using benzotriazol-**1**-yloxytris(dimethylamino)phosphonium hexafluorophosphate (BOP reagent), according to the procedure shown in Scheme 3. This procedure yielded mainly the symmetrical porphyrins resulting from the coupling of **A** with two **B** (17%) or **A** with two **C** (40%). The unsymmetrical porphyrin **8** (12%) was separated by chromatography on a reverse phase silica column using CH_3COOH/CH_3OH/H_2O, 1:1:2, as eluent.[34] Cleavage of the Pbf protective group followed by methylation of the pyridyl rings[15] yielded the water-soluble porphyrin MABAP.

Synthesis of BABAP

BABAP was obtained by the coupling of the porphyrin diacid with an excess of synthon **C**, in the presence of the BOP reagent, according to the procedure described in Scheme 4. The porphyrin precursor **10** was obtained in 48% yield. Cleavage of the Pbf protective groups followed by methylation yielded the bis-acridyl-bis-arginyl-porphyrin BABAP.

MABAP and BABAP were fully characterized by ^{1}H NMR spectroscopy and mass spectrometry (see Expt. Sect.). These techniques indicated that the acridine rings were neither methylated by methyl iodide, nor protonated at physiological pH.

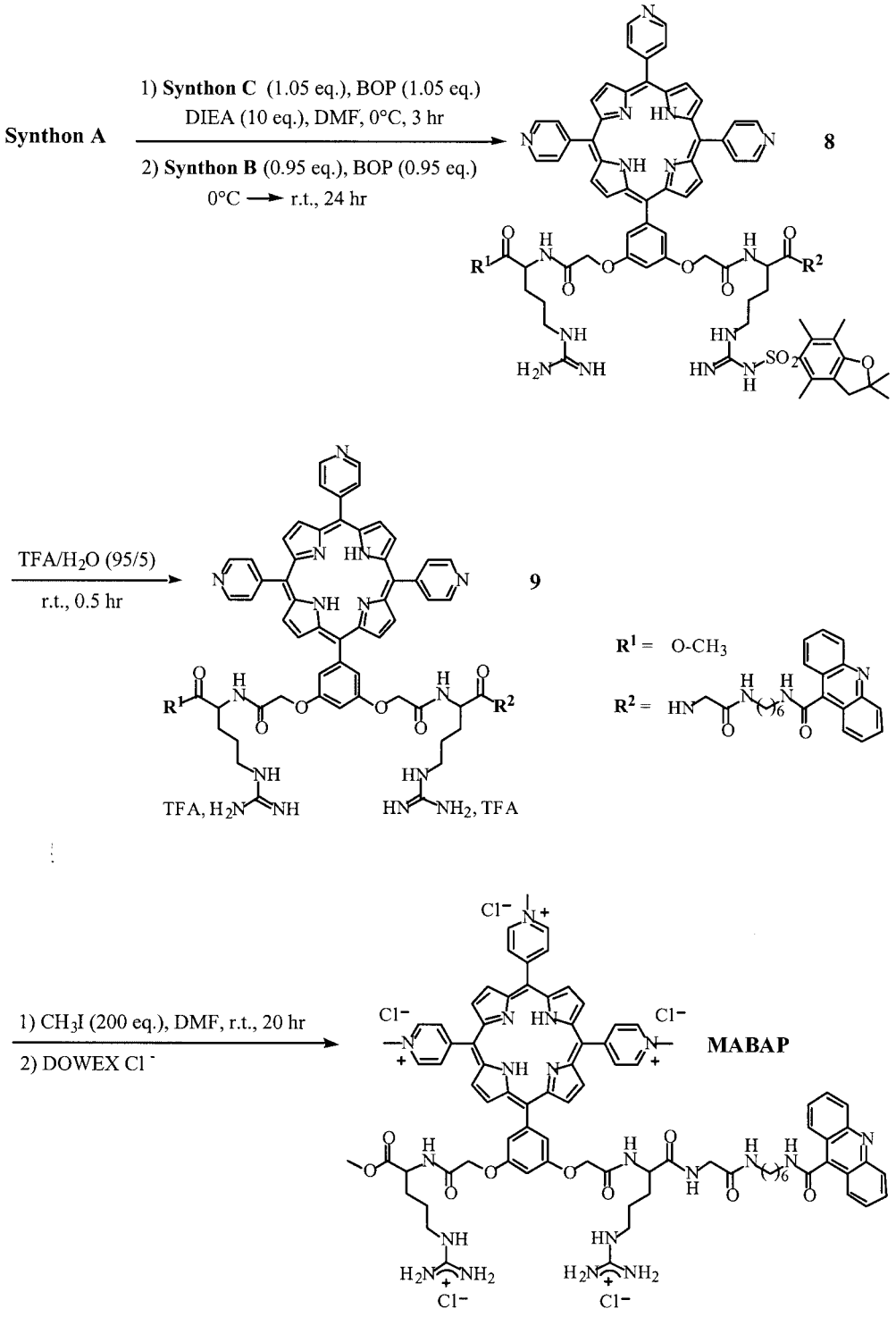

Scheme 3. Synthesis of MABAP

Binding of Bis-arginyl-porphyrin Derivatives to DNA

T_m Measurements

Thermal denaturation studies were performed on the dodecanucleotide d(TC GGGC GCCC GA)$_2$ alone and in the presence of BAP, MABAP and BABAP. d(TC GGGC GCCC GA)$_2$ is the central sequence of the oligonucleotide that we have modelled in the presence of the BAP derivatives. The normalized melting curves are given in Figure 5 (a) and the data are reported in Table 3. At a NaCl concentration of 100 mM, the thermal denaturation of this G-C rich dodecanucleotide alone occurs at a very high temperature (68 °C). As a result, and similar to our previous findings,[21] the amount of BAP-induced stabilization is very

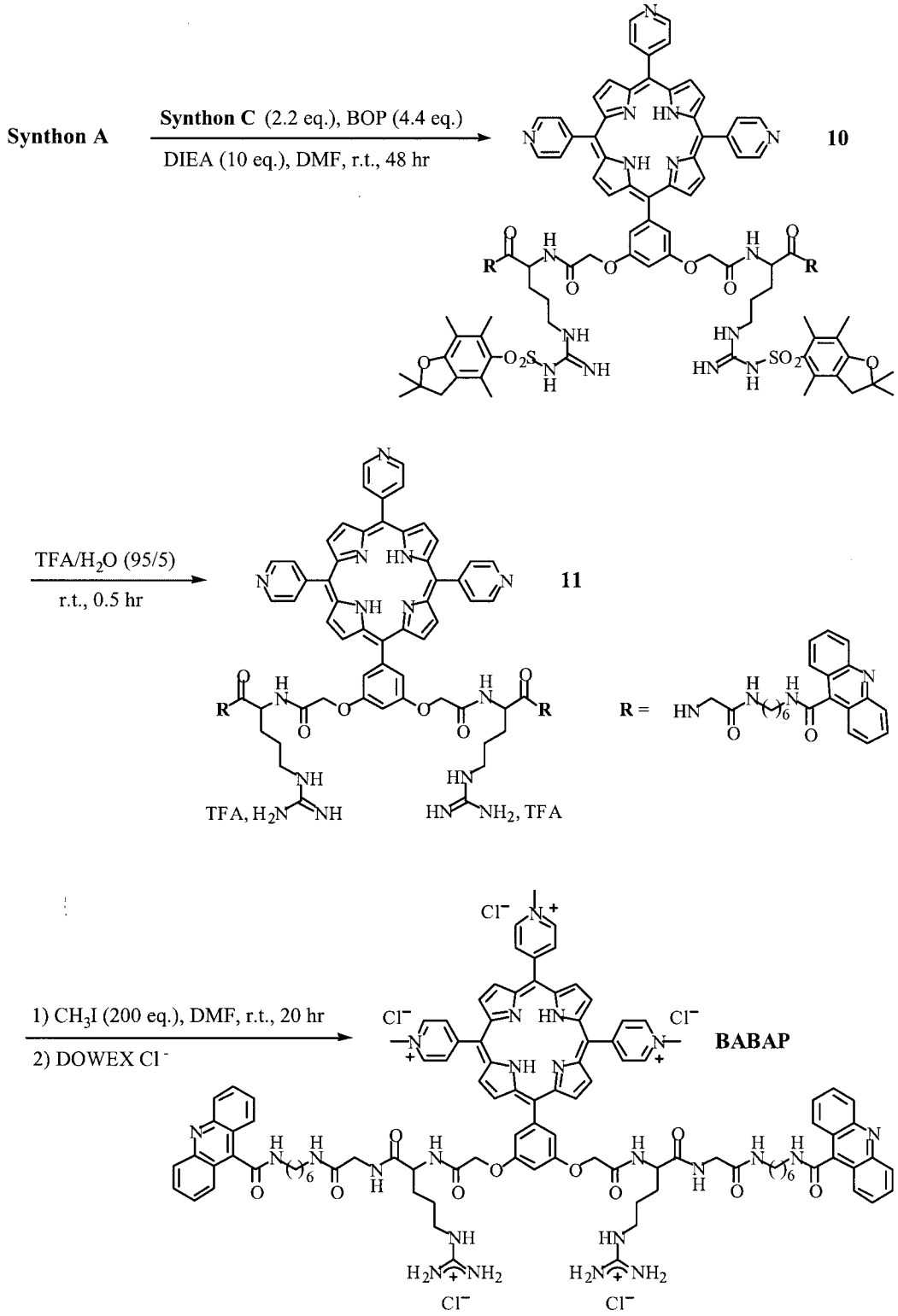

Scheme 4. Synthesis of BABAP

small (ΔT_m = 1 °C) [with the shorter decanucleotide d(GTGGC GCCAC)$_2$ that has a T_m of 56 °C, ΔT_m = 4 °C[21]]. MABAP produces no more stabilization than BAP. However, in the case of BABAP, we did not observe the beginning of a plateau, which corresponds to the absorbance of single-strand DNA, even at 90 °C, in contrast to the absorbance of the BAP- and MABAP-bound oligonucleotides. To lower the T_m value, we repeated the thermal denaturation studies in 10 mM NaCl, which resulted in a T_m value of 50 °C for the oligonucleotide alone. Under these

Table 3. Melting temperature of d(TC GGGC GCCC GA)$_2$ and d(TC GTAC GTAC GA)$_2$ in the presence of BAP, MABAP and BABAP [Oligonucleotide(bp)]/[Ligand] = 12

	d(TCGGGCGCCCGA)$_2$ 100 mM NaCl T_m (°C)	d(TCGGGCGCCCGA)$_2$ 10 mM NaCl T_m (°C)	d(TCGTACGTACGA)$_2$ 100 mM NaCl T_m (°C)
No ligand	68	50	48
BAP	69	66	50
MABAP	69	65	52
BABAP	n.d. probably > 78	56, 80	60

conditions the BAP and MABAP-bound oligonucleotides had T_m values of 66 and 65 °C, respectively, an increase of 16 and 15 °C. At this point we have no explanation for the virtually equal ΔT_m values of the BAP and MABAP complexes of this dodecanucleotide. The curve of the BABAP-bound oligonucleotide had a more complex behaviour, with two inflexion points at 56 and 80 °C. The latter corresponds to a ΔT_m of 30 °C (Figure not shown). Because of such complex behaviour, we repeated these experiments with another dodecanucleotide, d(TC GTAC GTAC GA)$_2$, which has fewer hydrogen bonds, and thus a lower melting temperature, namely 48 °C [Figure 5 (b)]. In this case, its BAP-, MABAP-, and BABAP-bound complexes had T_m values of 50, 52, and 60 °C, respectively. We consider this finding to be a clear indication of the increased DNA stabilization upon passing from mono- to bis- and tris-intercalation. Nevertheless, a stabilization of 12 °C for this oligonucleotide is low relative to the stabilization observed in the BABAP-d(TC GGGC GCCC GA)$_2$ complex. This suggests that BABAP stabilizes GGC GCC more than TAC GTA sequences. Finally we note that the 2 °C BAP-induced thermal stabilization is much smaller than the 4 °C one found for the sequence d(GTGGC GCCAC)$_2$ yet the latter has a higher T_m of 56 °C.[21] This is an additional indication for the intrinsic preference of BAP for sequences having a d(GGC GCC)$_2$ central core.

In order to complement these T_m measurements, we have also undertaken a combination of circular dichroism (CD) and topoisomerisation experiments to demonstrate the intercalation of the acridine rings of MABAP and BABAP in DNA.

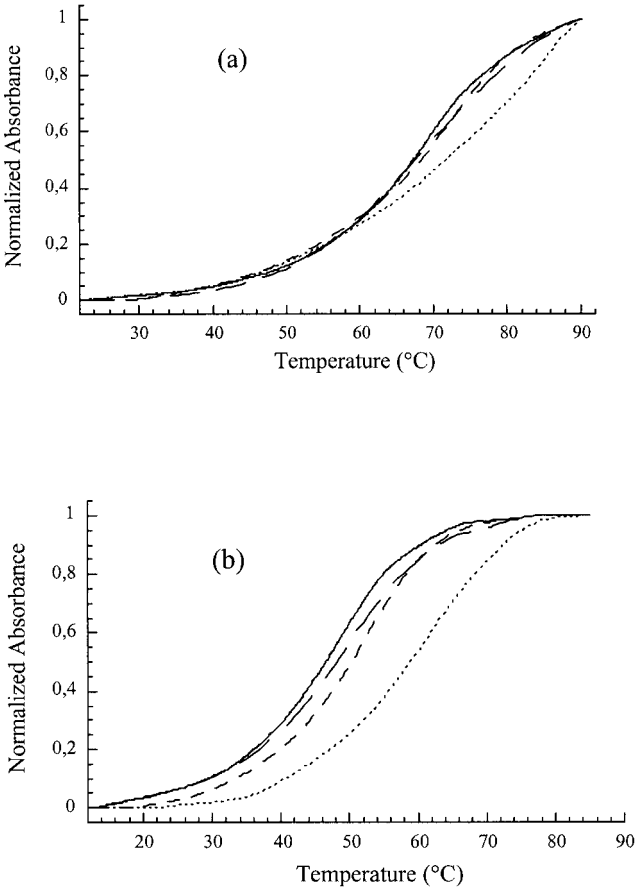

Figure 5. UV melting curves for (a) d(TC GGGC GCCC GA)$_2$ and (b) d(TC GTAC GTAC GA)$_2$ alone (-) and in the presence of BAP (— —), MABAP (---) and BABAP (···); [Oligonucleotide](bp)/[Ligand] = 12

Circular Dichroism

Intercalation of porphyrins is characterized by the appearance of a negative induced circular dichroism band in the Soret region (420−480 nm), the appearance of a positive induced band being indicative of a non-intercalated binding mode.[16a] The acridine moiety in MABAP and BABAP has a strong absorption band at 250 nm and a weak absorption band at 360 nm, and its binding to DNA will induce CD signals in both regions. However, as spectral changes in short-wavelength region could result either from a conformational change in the DNA upon binding of the ligand or from induced circular dichroism of the bound acridine, we have investigated only the longer wavelength region. As demonstrated by Wirth et al. and Gimenez-Arnau et al., the appearance of a weak and broad positive CD signal in the 350−400 nm region is indicative of the intercalation of the acridine ring.[35]

Our experiments were carried out on CT-DNA, synthetic polynucleotides and oligonucleotides with variable GC contents. We present here the interactions of BAP, MABAP and BABAP with poly(dG-dC)$_2$ and the central fragment d(TC GGGC GCCC GA)$_2$ of the oligonucleotide that we have modelled.

As seen in Figure 6 (a and b), the three porphyrins display a broad negative signal in the Soret region, the signature of the intercalation of the porphyrin ring in the polynu-

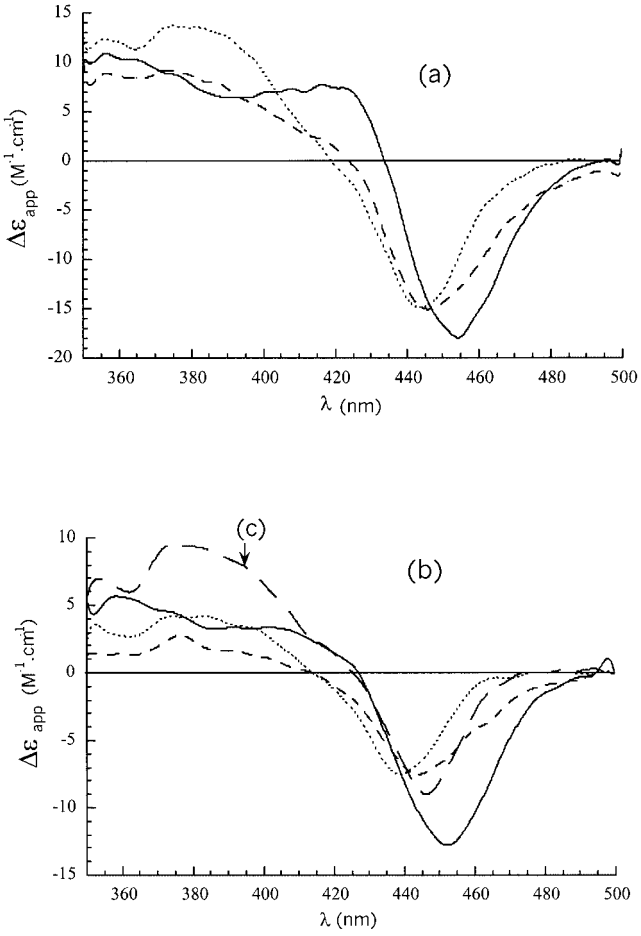

Figure 6. Induced circular dichroism (ICD) of BAP (-), MABAP (---) and BABAP (···) in the presence of (a) poly(dG-dC)$_2$, [DNA](bp)/[Ligand] = 30; (b) d(TC GGGC GCCC GA)$_2$, [DNA](bp)/[Ligand] = 12; (c) ICD of BABAP in the presence of d(TC GTAC GTAC GA)$_2$, [DNA](bp)/[BABAP] = 12

cleotide and the dodecamer. The weak and broad positive induced band around 380 nm in the MABAP and BABAP spectra contrasts with the corresponding monotonous decrease of the band in the 360−380 nm region in the case of the BAP complex. This could indicate that the acridines are intercalated. This band is more intense in the induced CD spectra of BABAP than in those of MABAP. This is in agreement with the bis-intercalation of the acridines in the BABAP complexes. These experiments were also performed on the dodecanucleotide d(TC GTAC GTAC GA)$_2$ investigated in the thermal denaturation studies. In the BABAP-d(TC GTAC GTAC GA)$_2$ complex [curve (c) represented in Figure 6 (b)], the induced acridine signal is more intense. This could reflect a facilitated intercalation due to the greater flexibility of this oligonucleotide.

Topoisomerase I-Uunwinding Experiments

Topoisomerase I catalyzes the relaxation of supercoiled plasmid DNA (form I_S) into the I_R form. In the presence of intercalators, the topology of DNA is modified and the topoisomerisation provides relaxed DNA with a smaller linking number.[36] After extraction, DNA gel electrophoresis shows topoisomers having mobilities intermediate between the relaxed (I_R) DNA (or the nicked form II also present in the native DNA) and the native supercoiled (I_S) DNA. This method allows to demonstrate the intercalation of ligands in DNA and the efficiency of the intercalation.

Figure 7 shows the results of the unwinding of a pTZ plasmid DNA in the presence of BAP, MABAP and BABAP. In these experiments, DNA was preincubated with topoisomerase I and increasing amounts of each of the three porphyrin compounds were added. At low porphyrin concentrations (lane 11), DNA had the same migration as relaxed DNA (I_R) (lane 3). Increasing amounts of added ligand provided topoisomers with increasing numbers of negative supercoils, which have increasing mobilities intermediate between those of relaxed and supercoiled DNA. A ligand-dependent concentration could be characterized for which most topoisomers migrate like supercoiled DNA, which indicates ligand-induced modification of the topology of topoisomerase I relaxed DNA. This occurred in lane 7 for BAP, lane 8 for MABAP and lane 9 for BABAP. The corresponding ligand concentrations provide information on the extent of ligand intercalation. These corresponded to [DNA](bp)/[Ligand] ratios ($1/r_0$) of 8 for BAP, 12 for MABAP and 24 for BABAP. The concentrations of MABAP and BABAP were thus 1.5- and three-times lower than the corresponding BAP concentration. These results are consistent with the involvement of the acridine rings in DNA binding, which, according to the modelling computations, should occur by intercalation.

Conclusion and Perspectives

We have resorted to molecular modelling to design mono- and bis-acridyl derivatives of the bis-arginyl porphyrin mono-intercalator BAP, denoted as MABAP and BABAP respectively. It was necessary to find an appropriate connector between the Arg backbone and the added acridine ring(s) that would enable the ring(s) to intercalate between DNA base pairs. This was a prerequisite to the chemical synthesis reported in this paper. In the absence of available experimental (X-ray or NMR) structural data, the computations reported here suggest the existence of several possibilities for complex formation between MABAP and BABAP and d(CTGTTC GGGC GCCC GAACAG)$_2$. The most stable complexes have both Arg side-chains in the major groove, bound to O^6/N^7 of the two successive G bases on a given strand upstream from the intercalation site. Those complexes having three, one, or two *N*-methylpyridinium rings in the minor groove are denoted by ′A′, ′B′, and ′C′, respectively. For a given Gly−C_6−Acr extension, those complexes in which the Gly−C_6 chain remains in the major groove or winds across the sugar-phosphate chain to reach the minor groove are denoted by ′I′ (internal) or ′E′ (external). The acridine ring intercalates from the major or the minor groove in these complexes respectively. As deduced fom the present calculations, the most stable complex

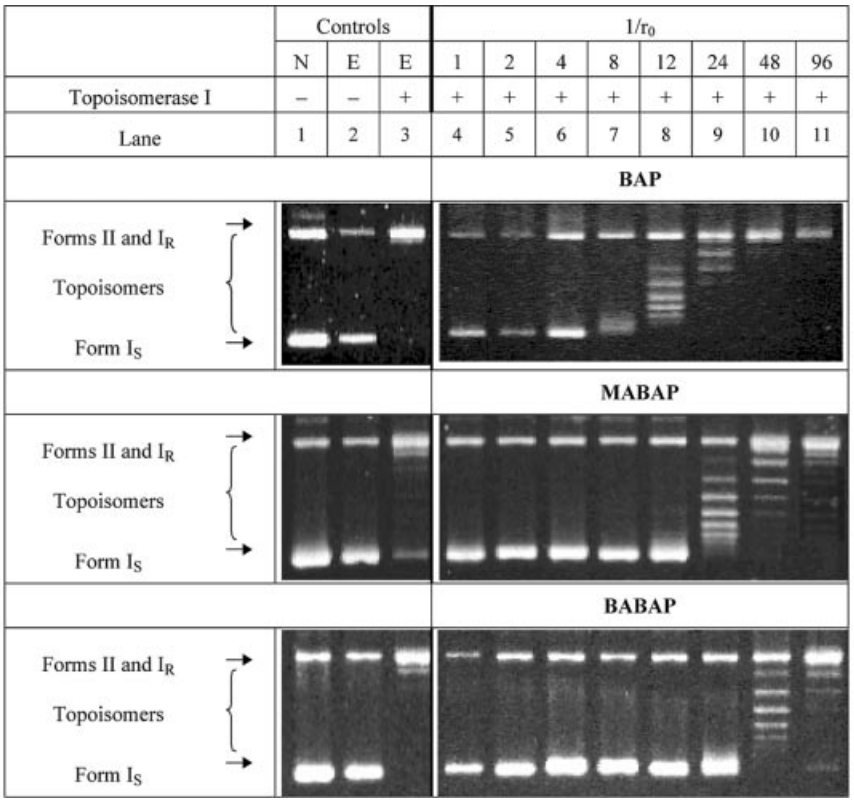

Figure 7. Topoisomerase I-unwinding of supercoiled DNA, incubated in the presence of increasing amounts of BAP, MABAP and BABAP. N: native DNA, E: extracted DNA. $1/r_0$ = [DNA](bp)/[Ligand]

is C-I, followed by complexes A-I and B-I for MABAP, and A-II, followed by complexes B-EE, C-II and B-IE for BABAP. The preference of the B complex for the EE mode can be understood by the fact that sliding the porphyrin ring along the diad axis allows the two arms to move more freely and reach the sugar-phosphate backbone than in mode A which restricts their mobility in the major groove.

Circular dichroism and topoisomerase I-unwinding experiments support the bis- and tris-intercalation of MABAP and BABAP in DNA. Furthermore, thermal denaturation studies have shown the melting temperatures of double-stranded oligonucleotides to be significantly higher in the presence of BABAP than in the presence of the mono-intercalator BAP.

The present calculations imply that substantial of A versus B as well as I versus E preferences could be achieved by modifying the nature as well as the length of the connector. This could be important from the perspective of replacing the acridine ring (which is mutagenic) by derivatives such as *m*-amsacrine (which is antitumoral). Thus compounds in which the $-NHSO_2CH_3$ substituent protrudes into the minor groove or the major groove could be tailored by modifying the nature of the Arg arms and their connectors to the added intercalators. In the present work, we have used 9-carboxyacridine, rather than a cationic 9-aminoacridine to provide additional intercalating groups because we wanted the porphyrin to intercalate in the $d(CpG)_2$ site prior to intercalation of the acridine. It has been shown by Ishikawa et al.[25d] that in cationic porphyrin-9-aminoacridine hybrids, intercalation of the acridine actually occurred at the expense of that of the porphyrin ring, although this could have been due to the rather short length of the connector arm. Synthesis of derivatives in which the acridines are connected to the linker by an NH, rather than a C=O group is underway in our laboratory (Ramiandrasoa et al., to be published). This should afford acridine protonation at neutral pH, thereby enhancing DNA binding, provided that porphyrin intercalation is not prevented. Derivatives with longer porphyrin-acridine connectors will be designed to facilitate tris-intercalation without excessive DNA distortion that could penalize the more rigid GC-rich sequences. The design and synthesis of BABAP thus constitutes a starting point in the design of tris-intercalating compounds that have three anchoring points, each of which has intrinsic antitumour properties, and whose connecting arms should be responsible for both sequence-specific recognition and modulatable II versus EE binding modes.

Experimental Section

General Methods: Coupling reactions were performed under an argon atmosphere and in a commercial acid- and base-free DMF (99.8% Aldrich). Most of the reactions were carried out in the dark. THF and dioxane were dried over sodium and distilled prior to use. All commercially available chemical reagents were used without purification. Reactions were monitored by thin layer chroma-

tography (TLC) performed on silica gel sheets containing UV fluorescent indicator (60 F_{254} Merck). ^{1}H and ^{13}C NMR spectra were recorded on Bruker AC 200, Bruker AC 250 and Bruker AC 400 spectrometers (200, 250 and 400 MHz for ^{1}H, respectively, and 50, 63 and 100 MHz for ^{13}C, respectively). Chemical shifts, δ, are reported in ppm taking residual $CHCl_3$ or CHD_2OD as the reference. Infrared spectra were recorded on a Bruker IFS 66 Fourier Transform spectrophotometer and UV/Visible spectra on a Safas 190 DES spectrophotometer. Mass spectra were recorded either on a Riberg Mag R10−10 or a Finningan-MAT-95-S. Elemental analyses were performed by the Service Central de Microanalyse du CNRS.

Computational Procedure: We have used the JUMNA 10 molecular mechanics procedure.[37] Similar to our previous studies devoted to porphyrin-oligopeptide conjugates, solvation effects were implicitly accounted for by the use of a sigmoidal dielectric function, and, to account for screening effects, the phosphodiester group had a net charge of −0.5.[19,21] Using the JUMNA procedure we generated two and three intercalation sites for bis- and tris-intercalating derivatives respectively. We then followed a similar strategy to that used in these previous studies, which involved a succession of constrained and unconstrained energy-minimization steps in which the DNA was first held rigid and then relaxed.[19,21] The distances between the amino groups of the Arg side-chains and the O^6/N^7 sites of the targeted bases were constrained as well as the distances between the N^1 and C^4 and C^5 atoms of the acridine and the nitrogens of the G and C bases of the corresponding acridine intercalation sites. The latter constraint is obviously necessary to ensure that the acridine rings overlap properly with the bases of the intercalation sites in the initial energy-minimization steps. Several simulations involving rigid or relaxed DNA with or without distance constraints were performed in parallel, and all ended up with relaxed DNA and unconstrained ligand minimization.

Molecular dynamics studies were carried out using the Cff91 forcefield and the Accelrys package. The DNA-BABAP complex was immersed in a water box of 3744 water molecules, and periodic boundary conditions were applied. No explicit counterions were included, but the phosphate charges were set to −0.5. To avoid distortions of DNA in the course of dynamics simulations, the hydrogen bonds between the base pairs were enforced by a harmonic restraining potential. Three different dynamics simulations were run at 300 K. In the first, DNA was held rigid, in the second, one DNA strand was relaxed and in the third, the two strands were relaxed. Starting from the JUMNA structure for complex A-II, energy minimization was first carried out with the conjugate gradient algorithm. Dynamics simulations were then initialized for 5 ps, and resumed during 100 ps, with frames recorded every 5 ps and subjected to energy minimization.

DNA Solutions: Oligonucleotides were purchased from Cybergène (France). They were dissolved in ultra-pure water and their concentrations, expressed in bases, were determined by measuring the absorbance at 260 nm at 90 °C, applying the following molar extinction coefficients (in $M^{-1}\cdot cm^{-1}$): d(TCGGGCGCCCGA): 7758; d(TCGTACGTACGA): 9975.[38] Poly(dG-dC)$_2$ (from Amersham Pharmacia Biotech) was dissolved in phosphate buffer (1 mL, pH 7) containing phosphate (25 mM) and NaCl (150 mM). Its concentration in base pairs (bp) was determined spectrophotometrically at 255 nm using a molar extinction coefficient of $1.68 \times 10^4\ M^{-1}\cdot cm^{-1}$.[39] Supercoiled pTZ plasmid (2861 base pairs) was isolated from JM109 *Escherichia coli* by the alkaline lysis method and purified using a Hybaid plasmid maxi kit. The concentration of DNA in base pairs was determined spectrophotometrically at 260 nm using a molar extinction coefficient of $1.31 \times 10^4\ M^{-1}\cdot cm^{-1}$.[40]

Oligonucleotide Thermal Denaturation Measurements: Optical thermal denaturation measurements were performed in quartz cuvettes (1 mL, 10 mm path length) on a Kontron Uvikon 933 spectrophotometer. The temperature of the cell holder was varied from 10 °C to 90 °C (0.15 °C min^{-1}) by circulating water using a Huber water bath, controlled by a Huber PD415 temperature programmer. Oligonucleotides were dissolved in sodium cacodylate buffer (10 mM, pH 7), containing NaCl (10 mM or 100 mM). Thermal denaturation curves of the complexes were measured at an oligonucleotide(base pair):ligand ratio of 12. The oligonucleotide concentration, in base pairs, was 2×10^{-5} M. The thermal denaturation profiles of the free duplexes and of the complexes were monitored at 260 nm. Melting temperatures (T_m) were determined from the first derivative of the melting curves.

Circular Dichroism: Circular dichroism spectra were recorded on a Jobin Yvon CD6 autodichrograph in a room thermostatted at 20 °C. All the measurements were made in sodium cacodylate buffer (10 mM, pH 7) containing NaCl (100 mM). A 3 mL, 10 mm path-length quartz cuvette was used to avoid dichroic effects from the cuvette. The spectra shown in this study were recorded at a DNA-(base pair):ligand ratio of 30 for poly(dG-dC)$_2$ and 12 for the dodecanucleotides. They were obtained by an average of four accumulations recorded with steps of 0.2 nm and a response time of 0.2 s. For each measurement, the spectrum of the porphyrin derivative at the same concentration in the same buffer and same cuvette was subtracted. The observed Δ(O.D.) was divided by the initial porphyrin concentration to give the apparent Δε values, $\Delta\varepsilon_{app}$.

Topoisomerisation Experiments: Reaction mixtures containing pTZ supercoiled plasmid (ca. 250 ng, final concentration in bp 0.265 μM), an aqueous solution of porphyrin derivative of known concentration (5 μL), 10X topoisomerase buffer (2 μL) and deionized water (up to 19 μL), were incubated for 5 min at 37 °C. Topoisomerase I (1 μL, 1 $u\cdot\mu L^{-1}$) was then added and the reaction mixture incubated for 30 min at 37 °C. The topoisomerase I reaction was stopped by adding Proteinase K (2.2 μL, 500 $\mu g\cdot mL^{-1}$), EDTA (2 μL, 0.5 M, pH 8) and SDS (1 μL, 10%), and the mixture was then incubated for 30 min at 50 °C. The mixture was extracted with phenol/chloroform, and DNA was precipitated,[40] redissolved in TE (10 μL), and BBSE 6X (2 μL) was added. This plasmid solution (10 μL) was submitted to electrophoresis on a 1.3% agarose gel in TBE buffer in a refrigerated tank maintained at 6 °C. The running buffer was recirculated. A constant voltage of 8 $V\cdot cm^{-1}$ was applied for 200 min. The DNA was then visualized using the gel that had been stained for 20 min in an ethidium bromide solution (1 $\mu g\cdot mL^{-1}$). The gel was photographed under transillumination (312 nm).

Abbreviations: EDTA: Ethylenediaminetetracetic acid, sodium salt, 0.5 M, pH 8; SDS: sodium dodecyl sulfate, 10%; BBSE 6X: Bromophenol Blue, SDS, EDTA (100 μL Bromophenol Blue 2%, 250 μL SDS, 100 μL EDTA, 250 μL glycerol, 300 μL TE); TBE: Tris, Borate, EDTA; TE: Tris, EDTA.[40]

***tert*-Butyl *N*-(6-Aminohexyl)carbamate (1):** Di-*tert*-butyl dicarbonate [(Boc)$_2$O] (7.09 g, 32.5 mmol) was dissolved in freshly distilled dioxane (80 mL) and added dropwise over 8 h to a stirred solution of 1,6-diaminohexane (28.3 g, 244 mmol) in dioxane (250 mL) under argon. The mixture was stirred at room temp. for 3 days. The solution was filtered and the solid residue [*N*,*N*′-bis(*tert*-butoxycarbonyl)diaminohexane] was washed with diethyl ether (3 × 10 mL). The filtrate was concentrated in vacuo, and then water (250 mL)

was added to precipitate the residual *N*,*N*′-bis(*tert*-butoxycarbonyl)-diaminohexane. The precipitate was filtered and washed with water (3 × 10 mL). The filtrate, containing excess diamine and the desired product, was extracted with CH_2Cl_2 (4 × 50 mL). The CH_2Cl_2 solution was washed with water, dried over Na_2SO_4 and the solvent evaporated to give pure *tert*-butyl *N*-(6-aminohexyl)carbamate (**1**) (5.02 g, 23.2 mmol) in 71% yield [relative to $(Boc)_2O$]. ^{1}H NMR (250 MHz, $CDCl_3$): δ = 1.23 (m, 2 H), 1.32 (m, 8 H), 1.43 (s, 9 H), 2.67 (t, *J* = 6.7 Hz, 2 H), 3.10 (q, *J* = 6.5 Hz, 2 H), 4.55 (t unresolved, 1 H). ^{13}C NMR (63 MHz, $CDCl_3$): δ = 26.1 (CH_2), 26.2 (CH_2), 28.0 (CH_3), 29.6 (CH_2), 33.0 (CH_2), 40.0 (CH_2), 41.5 (CH_2), 78.2 (C),155.7 (C). MS (CI): *m*/*z* = 217 (M^+ + H). $C_{11}H_{24}N_2O_2$ (216.33): calcd. C 61.08, H 11.18, N 12.95, O 14.79; found C 61.01, H 11.02, N 12.73, O 15.02.

***N*-[*N*-(*tert*-Butoxycarbonyl)-6-aminohexyl]-9-acridinecarboxamide (2):** Diisopropylethylamine (DIEA) (1.42 mL, 8.16 mmol) was added to a suspension of 9-acridinecarboxylic acid hydrate (1.64 g, 6.8 mmol) and BOP (3.31 g, 7.48 mmol) in DMF (30 mL) and the resulting solution was stirred for 20 min. *tert*-Butyl *N*-(6-aminohexyl)carbamate (**1**) (1.47 g, 6.8 mmol) was added and the reaction mixture was stirred for 24 h at room temp. The crude product was concentrated under reduced pressure and the residue was dissolved in acetone (20 mL) and added dropwise to a stirred solution of 5% $NaHCO_3$ (200 mL), according to the procedure previously developed by Kossanyi et al.[41] The mixture was allowed to stand for 24 h at room temp. This afforded a precipitate that was filtered, washed with water and dried to give **2** (2.19 g, 5 mmol, 74%) as a pale yellow powder. ^{1}H NMR (200 MHz, $CDCl_3$): δ = 1.33 (s, 9 H), 1.36 (m, 8 H), 3.16 (q, *J* = 6.4 Hz, 2 H), 3.67 (q, *J* = 6.4 Hz, 2 H), 4.51 (t unresolved, 1 H), 6.48 (t unresolved, 1 H), 7.50 (t, *J* = 7.8 Hz, 2 H), 7.72 (t, *J* = 7.8 Hz, 2 H), 7.96 (d, *J* = 7.8 Hz, 2 H), 8.10 (d, *J* = 7.8 Hz, 2 H). ^{13}C NMR (63 MHz, $CDCl_3$): δ = 26.9 (CH_2), 27.3 (CH_2), 28.7 (CH_3), 29.8 (CH_2), 30.4 (CH_2), 40.6 (CH_2), 40.8 (CH_2), 79.6 (C), 123.1 (C), 126.0 (CH), 127.5 (CH), 129.0 (CH), 131.6 (CH), 143.1 (C), 148.9 (C), 157.8 (C), 168.4 (C). MS (HRMS, *m*/*z* calcd. for $C_{25}H_{31}N_3O_3Na$): calcd. 444.22631; found 444.22610. $C_{25}H_{31}N_3O_3{\cdot}H_2O$ (439.56): calcd. C 68.31, H 7.57, N 9.56, O 14.56; found C 67.71, H 7.64, N 9.51, O 14.28.

***N*-(6-Aminohexyl)-9-acridinecarboxamide, TFA Salt (3):** *N*-[*N*-(*tert*-Butoxycarbonyl)-6-aminohexyl]-9-acridinecarboxamide (**2**) (270 mg, 0.64 mmol) was dissolved in TFA/CH_2Cl_2 (v/v, 4 mL) and the resulting solution was stirred at room temp. for 1 h. The solvent and most of the trifluoroacetic acid were removed under reduced pressure to give a brown gum, which upon trituration with diethyl ether (2 × 10 mL) yielded a yellow solid. The solid was dried under reduced pressure to afford the crude TFA salt **3** (277 mg, 99%) which was used in the next step without further purification. ^{1}H NMR (250 MHz, CD_3OD): δ = 1.56 (m, 4 H), 1.72 (m, 2 H), 1.82 (m, 2 H), 2.97 (t, *J* = 7.3 Hz, 2 H), 3.68 (t, *J* = 6.8 Hz, 2 H), 7.76 (t, *J* = 8.8 Hz, 2 H), 8.02 (t, *J* = 8.8 Hz, 2 H), 8.15 (d, *J* = 8.8 Hz, 2 H), 8.26 (d, *J* = 8.8 Hz, 2 H). ^{13}C NMR (50 MHz, CD_3OD): δ = 27.1 (CH_2), 27.7 (CH_2), 28.5 (CH_2), 30.1 (CH_2), 40.6 (CH_2), 40.8 (CH_2), 123.7 (C), 126.7 (CH), 128.4 (CH), 128.7 (CH), 133.0 (CH), 145.0 (C), 148.7 (C), 168.8 (C). MS (ES^+): *m*/*z* found: 322.1 (M^+ + H).

***N*-{*N*-[*N*-(*tert*-Butoxycarbonyl)glycyl]-6-aminohexyl}-9-acridinecarboxamide (4):** DIEA (436 μL, 2.5 mmol) was added to a stirred solution of *N*-(6-aminohexyl)-9-acridinecarboxamide, trifluoroacetate salt (**3**) (222 mg, 0.51 mmol) in DMF (2 mL). Simultaneously, a mixture of *N*-(*tert*-butoxycarbonyl)glycine (107 mg, 0.61 mmol), PyBOP (382 mg, 0.73 mmol) and DIEA (127 μL, 0.73 mmol) in DMF (2 mL) was stirred for 15 min to allow the formation of the activated ester. The solution of **3** was then added and the reaction mixture was stirred for 48 h at room temp. The crude product was concentrated under reduced pressure and the residue was dissolved in acetone (25 mL) and added dropwise to a stirred solution of 5% $NaHCO_3$ (250 mL). Treatment of the crude product by a solution of 5% $NaHCO_3$ as for **2** afforded acridinecarboxamide **4** (194 mg, 0.41 mmol) in 80% yield. ^{1}H NMR (250 MHz, $CDCl_3$): δ = 1.34 (s, 9 H), 1.40 (m, 6 H), 1.67 (m, 2 H), 3.12 (q, *J* = 6.3 Hz, 2 H), 3.55 (m, 4 H), 5.28 (t unresolved, 1 H), 6.39 (t unresolved, 1 H), 7.28 (t unresolved, 1 H), 7.38 (t, *J* = 8.8 Hz, 2 H), 7.61 (t, *J* = 8.8 Hz, 2 H), 7.81 (d, *J* = 8.8 Hz, 2 H), 7.97 (d, *J* = 8.8 Hz, 2 H). ^{13}C NMR (50 MHz, $CDCl_3$): δ = 27.5 (CH_2), 27.8 (CH_2), 28.7 (CH_3), 30.3 (CH_2), 30.4 (CH_2), 40.2 (CH_2), 40.9 (CH_2), 44.6 (CH_2), 80.6 (C), 123.6 (C), 126.5 (CH), 128.1 (CH), 129.5 (CH), 132.3 (CH), 143.9 (C), 149.5 (C), 158.2 (C), 168.4 (C), 172.4 (C). IR (KBr): $\tilde{\nu}$ = 3261, 2932, 1707, 1677, 1644, 1518, 1279, 1168 cm^{-1}. MS (ES^+): *m*/*z* found 501.5 (M^+ + Na). $C_{27}H_{34}N_4O_4$ (478.60): calcd. C 67.76, H 7.16, N 11.71; found C 67.81, H 7.38, N 11.37.

***N*-[*N*-(Glycyl)-6-aminohexyl]-9-acridinecarboxamide, TFA Salt (5):** Dissolution of acridinecarboxamide **4** (141 mg, 0.29 mmol) in TFA/CH_2Cl_2 (v/v, 3 mL) followed by the same treatment as applied to **2** afforded the crude TFA salt **5** (143 mg, 0.29 mmol) which was used in the next step without further purification. ^{1}H NMR (250 MHz, CD_3OD): δ = 1.61 (m, 6 H), 1.78 (m, 2 H), 3.35 (s, 2 H), 3.65 (m, 4 H), 7.69 (t, *J* = 8.8 Hz, 2 H), 7.91 (t, *J* = 8.8 Hz, 2 H), 8.07 (d, *J* = 8.8 Hz, 2 H), 8.21 (d, *J* = 8.8 Hz, 2 H). ^{13}C NMR (63 MHz, CD_3OD): δ = 27.5 (CH_2), 27.8 (CH_2), 30.2 (CH_2), 30.3 (CH_2), 40.5 (CH_2), 40.8 (CH_2), 41.4 (CH_2), 123.7 (C), 126.5 (CH), 128.1 (CH), 129.6 (CH), 132.3 (CH), 145.2 (C), 149.6 (C), 167.1 (C), 171.2 (C). MS (ES^+): *m*/*z* found 379.2 (M^+ + H).

***N*-(*N*-{*N*-[N^{α}-Fluoren-9-ylmethoxycarbonyl-N^{η}-(2,2,4,6,7-pentamethyldihydrobenzofuran-5-sulfonyl)arginyl]glycyl}-6-aminohexyl)-9-acridinecarboxamide (6):** A mixture of Fmoc-Arg(Pbf)-OH (100 mg, 0.15 mmol), BOP (79 mg, 0.18 mmol) and DIEA (31 μL, 0.18 mmol) in DMF (4 mL) was stirred at room temp. for 15 min, then cooled to 0 °C. Acridinecarboxamide **5** (74 mg, 0.15 mmol) and DIEA (130 μL, 0.75 mmol) were dissolved in DMF (4 mL) and added dropwise to the activated ester of Fmoc-Arg(Pbf)-OH. This reaction mixture was stirred for 20 min at 0 °C, then at room temp. for 24 h. DIEA and DMF were evaporated under reduced pressure and the residue was dissolved in acetone (20 mL) and added dropwise to a stirred solution of 5% $NaHCO_3$ (200 mL). The mixture was allowed to stand for 24 h and the resulting precipitate was filtered, dried and purified by silica gel 60 (Merck, 40−63 μm) column chromatography (CH_2Cl_2/MeOH, 95:5) to afford compound **6** (109 mg, 0.11 mmol) in 70% yield. ^{1}H NMR (400 MHz, CD_3OD): δ = 1.40 [m, 10 H, $(CH_2)_2$ alkyl chain + 2 CH_3 Pbf], 1.50 (m, 4 H, C*H*$_2$CH$_2$NHGly + $CH_2\gamma$), 1.67 (m, 4 H, C*H*$_2$CH$_2$NHCOAcr + $CH_2\beta$), 2.05 (s, 3 H, CH_3 Pbf), 2.48 (s, 3 H, CH_3 Pbf), 2.55 (s, 3 H, CH_3 Pbf), 2.95 (s, 2 H, CH_2 Pbf), 3.14 (m, 4 H, C*H*$_2$NHGly + $CH_2\delta$), 3.55 (t, *J* = 6.8 Hz, 2 H, C*H*$_2$NHCOAcr), 3.70 (d, *J* = 16.8 Hz, 1 H, CH Gly), 3.88 (d, *J* = 16.8 Hz, 1 H, CH Gly), 3.95 (t, *J* = 7.8 Hz, 1 H, CHα), 4.19 (t, *J* = 6.8 Hz, 1 H, CH Fmoc), 4.37 (m, 2 H, CH_2 Fmoc), 7.28 (t, *J* = 7.5 Hz, 2 H, 2 CH Fmoc), 7.36 (t, *J* = 7.5 Hz, 2 H, 2 CH Fmoc), 7.63 (m, 4 H, 2 CH Fmoc + 2 CH Acr), 7.78 (d, *J* = 7.5 Hz, 2 H, 2 CH Fmoc), 7.85 (t, *J* = 8.1 Hz, 2 H, 2 CH Acr), 8.04 (d, *J* = 8.1 Hz, 2 H, 2 CH Acr), 8.17 (d, *J* = 8.1 Hz, 2 H, 2 CH Acr). ^{13}C NMR (100 MHz, CD_3OD): δ = 12.5 (CH_3), 18.4 (CH_3), 19.6 (CH_3), 26.9 (CH_2), 27.4 (CH_2), 27.7 (CH_2), 28.7 (CH_3), 30.2 (CH_2), 30.3 (CH_2), 30.9 (CH_2), 40.4 (CH_2), 40.8 (CH_2), 41.3

(CH_2), 43.6 (CH_2), 43.9 (CH_2), 48.0 (CH), 56.6 (CH), 68.0 (CH_2), 87.6 (C), 118.4 (C), 121.0 (CH), 123.7 (C), 126.0 (CH), 126.1 (CH), 126.6 (C), 128.2 (CH), 128.9 (CH), 129.6 (CH), 132.3 (CH), 133.5 (C), 134.3 (C), 139.4 (C), 142.6 (C), 143.9 (C), 145.1 (C), 149.6 (C), 158.1 (C), 158.8 (C), 169.0 (C), 171.4 (C). IR (KBr): $\bar{\nu}$ = 3340, 3064, 2930, 1703, 1648, 1549, 1255, 1105 cm^{-1}. MS [HRMS, *m*/*z* calcd. for $C_{56}H_{64}N_8O_8SNa$ (M^+ + Na)]: calcd. 1031.44743; found 1031.44655.

***N*-(*N*-{*N*-[*N*$^{\eta}$-(2,2,4,6,7-Pentamethyldihydrobenzofuran-5-sulfonyl)-arginyl]glycyl}-6-aminohexyl)-9-acridinecarboxamide (7):** DBU (52 µL, 0.35 mmol) was added to a solution of acridinecarboxamide **6** (91 mg, 0.09 mmol) in THF (2.6 mL) and the solution was stirred at room temp. for 15 min. The reaction mixture was poured into diethyl ether (100 mL) whilst stirring. The precipitate was filtered, washed with diethyl ether and dried. It was then dissolved in CH_2Cl_2 (50 mL) and the solution was washed with saturated aqueous NaCl solution (50 mL), then with water (3 × 50 mL), and dried over Na_2SO_4. After evaporation in vacuo, the acridinecarboxamide **7** (54 mg, 0.07 mmol) was obtained in 75% yield. ^{1}H NMR (400 MHz, CD_3OD): δ = 1.44 (s, 6 H, 2 CH_3 Pbf), 1.56 [m, 10 H, $(CH_2)_3$ alkyl chain + $CH_2\beta$ + $CH_2\gamma$), 1.78 (m, 2 H, C*H*$_2$CH$_2$NHCOAcr), 2.07 (s, 3 H, CH_3 Pbf), 2.49 (s, 3 H, CH_3 Pbf), 2.55 (s, 3 H, CH_3 Pbf), 2.98 (s, 2 H, CH_2 Pbf), 3.14 (m, 2 H, $CH_2\delta$), 3.24 (t, *J* = 6.8 Hz, 2 H, C*H*$_2$NHGly), 3.64 (t, *J* = 6.8 Hz, 2 H, C*H*$_2$NHCOAcr), 3.81 (d, *J* = 16.5 Hz, 1 H, CH Gly), 3.86 (d, *J* = 16.5 Hz, 1 H, CH Gly), 3.95 (m, 1 H, CHα), 7.68 (t, *J* = 8.8 Hz, 2 H, 2 CH Acr), 7.89 (t, *J* = 8.8 Hz, 2 H, 2 CH Acr), 8.07 (d, *J* = 8.8 Hz, 2 H, 2 CH Acr), 8.19 (d, *J* = 8.8 Hz, 2 H, 2 CH Acr). ^{13}C NMR (100 MHz, CD_3OD): δ = 12.5 (CH_3), 18.4 (CH_3), 19.6 (CH_3), 26.6 (CH_2), 27.5 (CH_2), 27.8 (CH_2), 28.7 (CH_3), 30.2 (CH_2), 30.3 (CH_2), 40.3 (CH_2), 40.9 (CH_2), 41.5 (CH_2), 43.3 (CH_2), 43.9 (CH_2), 55.6 (CH), 87.6 (C), 118.4 (C), 123.6 (C), 126.0 (CH), 126.5 (C), 128.1 (CH), 129.5 (CH), 132.3 (CH), 133.4 (C), 134.3 (C), 139.3 (C), 143.9 (C), 145.1 (C), 149.5 (C), 158.0 (C), 169.0 (C), 171.3 (C). MS [HRMS, *m*/*z* calcd. for $C_{41}H_{54}N_8O_6SNa$ (M^+ + Na)]: calcd. 809.37847; found 809.37792.

Porphyrin 8: Porphyrin diacid (synthon **A**) (36 mg, 0.047 mmol) was dissolved in DMF (2 mL) and the solution was stirred under argon at 0 °C. After complete dissolution, BOP (22 mg, 0.05 mmol) and DIEA (80 µL, 0.47 mmol) were added and the mixture was stirred for 0.5 h. Acridinecarboxamide **7** (39 mg, 0.05 mmol) was then added and the mixture was stirred in the dark for 3 h. L-Arginine methyl ester hydrochloride (11.5 mg, 0.044 mmol) and BOP (19.5 mg, 0.044 mmol) were then added and the mixture was stirred at room temp. for 24 h. After evaporation of the solvent, the residue was dissolved in acetone (5 mL) and the resulting solution was slowly added to 50 mL of water whilst stirring. The mixture was allowed to stand overnight at 6 °C. The resulting red precipitate was filtered off through a filter funnel (porosity 4) coated with Celite, then dissolved in CH_2Cl_2/MeOH, 95:5, and the solvent evaporated in vacuo. The crude product, consisting of a mixture of porphyrins, was passed through a reverse phase column Lichroprep RP-18 (40−63 µm) (AcOH/MeOH/H_2O, 1:1:2 then 2:1:2). Porphyrin **8** (10 mg, 5.75.10^{-3} mmol) was obtained in 12% yield. ^{1}H NMR (400 MHz, CD_3OD): δ = 1.52 [m, 16 H, $(CH_2)_4$ alkyl chain + 2 $CH_2\beta$ + 2 $CH_2\gamma$], 1.76 (s, 6 H, 2 CH_3 Pbf), 2.16 (s, 3 H, CH_3 Pbf), 2.27 (s, 3 H, CH_3 Pbf), 2.58 (s, 2 H, CH_2 Pbf), 2.90 (m, 4 H, 2 $CH_2\delta$), 3.04 (m, 2 H, C*H*$_2$NHGly), 3.34 (m, 2 H, C*H*$_2$NHCOAcr), 3.44 (s, 3 H, $COOCH_3$), 3.68 (m, 2 H, CH_2 Gly), 4.24 (m, 1 H, CHα), 4.37 (s, 2 H, C*H*$_2$OPh), 4.49 (m, 3 H, CHα + C*H*$_2$OPh), 6.81 (s, 1 H, CH Ph), 7.31 (m, 4 H, 4 CH Acr), 7.44 (m, 2 H, 2 CH Ph), 7.67 (d, *J* = 8.0 Hz, 2 H, 2 CH Acr), 7.81 (d, *J* = 8.0 Hz, 2 H, 2 CH Acr), 7.87 + 7.98 (m + d, 6 H, 6 CH pyridyl), 8.55−8.74 (br., 12 H, 8 CH pyrrole + 4 CH pyridyl), 8.86 (d, 2 H, 2 CH pyridyl). UV/Vis (CH_3OH): λ_{max} (% Abs) = 250 (53), 358 (8.3), 421 (100), 512 (1.6), 555 (4.2), 594 (1.2), 643 nm (0.3). MS (ES^+): *m*/*z* (%) = 1704.9 (100) (M^+ + H), 853.3 (26) (M^{2+} +2 H)/2, 569.2 (8) (M^{3+} +3 H)/3.

Porphyrin 10: A mixture of porphyrin diacid (synthon **A**) (17 mg, 0.022 mmol), BOP (44 mg, 0.10 mmol) and DIEA (40 µL, 0.23 mmol) in DMF (2 mL) was stirred for 1 h under argon. Acridinecarboxamide **7** (39 mg, 0.05 mmol) was then added and the reaction mixture was stirred for 48 h at room temp. After removal of DIEA and DMF under reduced pressure, the crude product was purified by silica gel (Polygoprep 6−12 µm) column chromatography (CH_2Cl_2/MeOH, 90:10) to afford the porphyrin **10** (26 mg, 0.011 mmol) in 48% yield. ^{1}H NMR (400 MHz, $CDCl_3$): δ = 1.28 [m, 20 H, 2 $(CH_2)_2$ alkyl chain + 4 CH_3 Pbf], 1.38 (m, 8 H, 2 C*H*$_2$CH$_2$NHGly + 2 $CH_2\gamma$), 1.52 (m, 4 H, 2 C*H*$_2$CH$_2$NHCOAcr), 1.61 (m, 2 H, 2 CHβ_1), 1.73 (m, 2 H, 2 CHβ_2), 1.88 (s, 6 H, 2 CH_3 Pbf), 2.30 (s, 6 H, 2 CH_3 Pbf), 2.38 (s, 6 H, 2 CH_3 Pbf), 2.75 (s, 4 H, 2 CH_2 Pbf), 2.91 (m, 4 H, 2 $CH_2\delta$), 3.12 (m, 4 H, 2 C*H*$_2$NHGly), 3.41 (m, 4 H, 2 C*H*$_2$NHCOAcr), 3.67 (d, *J* = 16.7 Hz, 2 H, 2 CH Gly), 3.78 (d, *J* = 16.7 Hz, 2 H, 2 CH Gly), 4.32 (m, 2 H, 2 CHα), 4.47 (d, *J* = 15.0 Hz, 2 H, 2 C*H*OPh), 4.56 (d, *J* = 15.0 Hz, 2 H, 2 C*H*OPh), 6.83 (s, 1 H, CH Ph), 7.27 (d, *J* = 2.4 Hz, 2 H, 2 CH Ph), 7.31 (m, 4 H, 4 CH Acr), 7.51 (m, 4 H, 4 CH Acr), 7.78 (d, *J* = 8.5 Hz, 4 H, 4 CH Acr), 7.93 (d, *J* = 8.5 Hz, 4 H, 4 CH Acr), 8.07 (d, *J* = 5.8 Hz, 4 H, 4 CH pyridyl), 8.10 (d, *J* = 5.8 Hz, 2 H, 2 CH pyridyl), 8.70 (br., 8 H, 8 CH pyrrole), 8.83 (d, *J* = 5.8 Hz, 4 H, 4 CH pyridyl), 8.87 (d, *J* = 5.8 Hz, 2 H, 2 CH pyridyl). UV/Vis (CH_3OH): λ_{max} (% Abs) = 250 (90), 360 (16), 415 (100), 511 (6.7), 544 (2.0), 587 (2.1), 644 nm (1.2). MS (ES^+): *m*/*z* (%) = 1152.4 (100) (M^{2+} + 2 H)/2, 768.6 (48) (M^{3+} + 3 H)/3.

Synthesis of Porphyrins 9 and 11 by Removal of the Pbf Protective Group: Porphyrin **8** (10 mg, 5.75 × 10^{-3} mmol) was dissolved in TFA/H_2O (95:5, 1 mL) and the resulting solution was stirred at room temp. for 0.5 h. Deprotection was monitored by reverse phase TLC (AcOH/MeOH/H_2O, 2:1:2). The solvents were removed under reduced pressure and the crude residue was dissolved in MeOH (2 mL). This solution was slowly added to Et_2O (50 mL) whilst stirring to afford porphyrin **9** as a red precipitate which was filtered and washed with Et_2O. Porphyrin **9** (9.6 mg, 5.7 × 10^{-3} mmol) was obtained in quantitative yield and was immediately used in the next step without further purification. Porphyrin **11** was obtained in quantitative yield from porphyrin **10** using the same procedure, and was immediately used in the next step without further purification.

Mono-acridyl-bis-arginyl-porphyrin (MABAP): A large excess of CH_3I (52 µL, 0.85 mmol) was added to a solution of porphyrin **9** (7 mg, 4.16 × 10^{-3} mmol) in DMF (6 mL). The mixture was stirred at 40 °C for 3 h. After removal of DMF and CH_3I under reduced pressure, the crude residue was dissolved in water (1 mL) and this solution was passed through a column of Dowex Cl^- ion exchange resin. The aqueous layer was evaporated and the product was precipitated in H_2O/acetone to afford MABAP (5 mg, 2.98 × 10^{-3} mmol) in 72% yield. ^{1}H NMR (400 MHz, CD_3OD): δ = 1.19−1.45 [m, 8 H, $(CH_2)_4$ alkyl chain], 1.64 (m, 4 H, 2 $CH_2\gamma$), 1.82 (m, 2 H, 2 CHβ_1), 1.94 (m, 2 H, 2 CHβ_2), 3.03 (m, 2 H, C*H*$_2$NHGly), 3.17 (m, 4 H, 2 $CH_2\delta$), 3.60 (m, 2 H, C*H*$_2$NHCOAcr), 3.54 (s, 3 H, $COOCH_3$), 3.71 (d, *J* = 16.6 Hz, 1 H, CH Gly), 3.88 (d, *J* = 16.6 Hz, 1 H, CH Gly), 4.41 (t, 1 H, CHα), 4.59 (m, 5 H, CHα + 2 C*H*$_2$OPh), 4.81 (s, 9 H, 3 N^+CH_3), 7.20 (s, 1 H, CH Ph), 7.25 (t, 1 H, CH Acr), 7.41 (t, 1 H, CH Acr), 7.46 (t, 1 H, CH Acr), 7.52 (t, 1 H, CH Acr), 7.58 (s, 1 H, CH Ph), 7.65 (m, 3 H, CH Ph + 2

CH Acr), 7.71 (d, 1 H, CH Acr), 7.85 (d, 1 H, CH Acr), 8.88 (d, 2 H, 2 CH pyridyl), 8.98 (m, 4 H, 4 CH pyridyl), 9.06−9.30 (br., 8 H, 8 CH pyrrole), 9.33 (d, 2 H, 2 CH pyridyl), 9.39 (d, 4 H, 4 CH pyridyl). UV/Vis (H_2O): λ_{max} (% Abs) = 252 (74), 361 (22.7), 434 (100), 556 (7.6), 644 nm (1.1). MS (ES^+): *m/z* (%) = 374.6 (100) (M^{4+} − 5 Cl − H)/4, 498.8 (53) (M^{3+} − 5 Cl − 2 H)/3, 299.7 (23) (M^{5+} − 5 Cl)/5.

Bis-acridyl-bis-arginyl-porphyrin (BABAP): A large excess of CH_3I (43 μL, 0.7 mmol) was added to a solution of porphyrin **11** (7 mg, 3.45×10^{-3} mmol) in DMF (6 mL). The mixture was stirred at 40 °C for 3 h. After removal of DMF and CH_3I under reduced pressure, the crude residue was dissolved in water (1 mL) and this solution was passed through a column of Dowex Cl^- ion exchange resin. The aqueous layer was evaporated and the product was precipitated in H_2O/acetone to afford BABAP (6 mg, 2.96×10^{-3} mmol) in 86% yield. ^1H NMR (400 MHz, CD_3OD): δ = 1.15 [m, 8 H, 2 $(CH_2)_2$ alkyl chain], 1.37 (m, 8 H, 2 CH_2CH_2NHGly + 2 $CH_2CH_2NHCOAcr$), 1.68 (m, 4 H, 2 $CH_2\gamma$), 1.90 (m, 4 H, 2 $CH_2\beta$), 2.99 (m, 4 H, 2 $CH_2\delta$), 3.12 (m, 4 H, 2 CH_2NHGly), 3.19 (m, 4 H, 2 $CH_2NHCOAcr$), 3.75 (d, *J* = 17.0 Hz, 2 H, 2 CH Gly), 3.83 (d, *J* = 17.0 Hz, 2 H, 2 CH Gly), 4.33 (m, 2 H, 2 CHα), 4.78 (s, 4 H, 2 CH_2OPh), 4.82 (s, 9 H, 3 N^+CH_3), 7.19 (m, 9 H, CH Ph + 8 CH Acr), 7.53 (m, 10 H, 2 CH Ph + 8 CH Acr), 8.94 (d, *J* = 5.6 Hz, 4 H, 4 CH pyridyl), 9.00 (d, *J* = 5.6 Hz, 2 H, 2 CH pyridyl), 9.15 (br., 8 H, 8 CH pyrrole), 9.35 (d, *J* = 5.6 Hz, 4 H, 4 CH pyridyl), 9.40 (d, *J* = 5.6 Hz, 2 H, 2 CH pyridyl). UV/Vis (H_2O): λ_{max} (% Abs) = 251 (100), 360 (21.3), 438 (73), 552 (9.0), 641 nm (0.5). MS (ES^+): *m/z* (%) = 461.1 (100) (M^{4+} − 5 Cl − H)/4, 614.1 (44) (M^{3+} − 5 Cl − 2 H)/3, 368.8 (19) (M^{5+} − 5 Cl)/5.

Acknowledgments

This work was supported by the Agence Nationale de Recherche sur le Sida (ANRS), which is personally acknowledged by one of us (A. K.) for financial support. We also thank the Ligue Nationale Contre le Cancer (Comité de Paris) for support. The molecular dynamics studies were done on the computers of CINES (Montpellier, France). Finally, we thank the Commissariat à l'Energie Atomique (CEA) and the Département d'Ingénierie des Protéines (Prof. A. Ménez) for access to their dichrograph.

[1] [1a] N. Zein, M. Poncin, R. Nilakantna, G. A. Ellestad, *Science* **1989**, *244*, 697−699. [1b] C. Zimmer, U. Wahnert, *Progr. Biophys. Mol. Biol.* **1986**, *41*, 31−112. [1c] M. Mrksich, W. S. Wade, T. J. Dwyer, B. H. Geierstanger, D. E. Wemmer, P. B. Dervan, *Proc. Natl. Acad. Sci. U. S. A.* **1992**, *89*, 7586−7590. [1d] T. J. Dwyer, B. H. Geierstanger, Y. Bathini, J. W. Lown, D. E. Wemmer, *J. Am. Chem. Soc.* **1992**, *114*, 5911−5919. [1e] S. N. Ho, S. H. Boyer, S. L. Schreiber, S. J. Danishefshky, G. R. Crabtree, *Proc. Natl. Acad. Sci. U. S. A.* **1994**, *91*, 9203−9207. [1f] V. A. Nikolaev, S. L. Grokhovsky, A. N. Surovaya, T. A. Leinsoo, N. Y. Sidorova, A. S. Zasedatelev, A. L. Zhuze, G. A. Strahan, R. H. Shafer, G. V. Gursky, *J. Biomol. Struct. Dyn.* **1996**, *14*, 31−47. [1g] H. Xuereb, M. Maletic, J. Gildersleeve, I. Pelczer, D. Kahne, *J. Am. Chem. Soc.* **2000**, *122*, 1883−1890. [1h] S. Neidle, *Nat. Prod. Rep.* **2001**, *18*, 291−309. [1i] P. B. Dervan, *Bioorg. Med. Chem.* **2001**, *9*, 2215−2235.

[2] [2a] F. Arcamone, *Doxorubicin, Anticancer Antibiotics,* Academic Press, New York, **1981**. [2b] S. H. Lee, I. H. Goldberg, *Biochemistry* **1989**, *28*, 1019−1026.

[3] [3a] C. Bailly, N. Helbecque, J.-P. Hénichart, P. Colson, C. Houssier, K. E. Rao, R. G. Shea, J. W. Lown, *J. Mol. Recognit.* **1990**, *3*, 26−35. [3b] C. Bailly, J.-P. Hénichart, *Bioconjugate Chem.* **1991**, *2*, 379−393. [3c] G. Anneheim-Herbelin, M. Perrée-Fauvet, A. Gaudemer, P. Hélissey, S. Giorgi-Renault, N. Gresh, *Tetrahedron Lett.* **1993**, *34*, 7263−7266. [3d] H. Goulaouic, S. Carteau, F. Subra, J.-F. Mouscadet, C. Auclair, J.-S. Sun, *Biochemistry* **1994**, *33*, 1412−1418. [3e] C. Bourdouxhe-Housiaux, P. Colson, C. Houssier, M. J. Waring, C. Bailly, *Biochemistry* **1996**, *35*, 4251−4264. [3f] P. Hélissey, C. Bailly, J. N. Vishwakarma, C. Auclair, M. J. Waring, S. Giorgi-Renault, *Anti-Cancer Drug Des.* **1996**, *11*, 527−551.

[4] [4a] H. E. Moser, P. B. Dervan, *Science* **1987**, *238*, 645−650. [4b] T. Le Doan, L. Perrouault, D. Praseuth, N. Habhoub, J.-L. Decout, N. T. Thuong, J. Lhomme, C. Hélène, *Nucleic Acids Res.* **1987**, *15*, 7749−7760. [4c] C. Hélène, J.-J. Toulmé, *Biochim. Biophys. Acta* **1990**, *1049*, 99−125. [4d] A. De Mesmaeker, R. Häner, P. Martin, H. E. Moser, *Acc. Chem. Res.* **1995**, *28*, 366−374. [4e] C. Escudé, C. H. Nguyen, J.-L. Mergny, J.-S. Sun, E. Bisagni, T. Garestier, C. Hélène, *J. Am. Chem. Soc.* **1995**, *117*, 10212−10219.

[5] J.-S. Sun, J.-C. François, T. Montenay-Garestier, T. Saison-Behmoaras, V. Roig, N. T. Thuong, C. Hélène, *Proc. Natl. Acad. Sci. U. S. A.* **1989**, *86*, 9198−9202.

[6] [6a] B. Hyrup, P. E. Nielsen, *Bioorg. Med. Chem.* **1996**, *4*, 5−23. [6b] P. E. Nielsen, *Acc. Chem. Res.* **1999**, *32*, 624−630.

[7] C. Park, J. L. Campbell, W. A. Goddard III, *J. Am. Chem. Soc.* **1995**, *117*, 6287−6291.

[8] B. Cuenoud, A. Scheparz, *Science* **1993**, *259*, 510−513.

[9] [9a] N. Y. Sardesai, K. Zimmerman, J. K. Barton, *J. Am. Chem. Soc.* **1994**, *116*, 7502. [9b] N. Y. Sardesai, J. K. Barton, *J. Biol. Inorg. Chem.* **1997**, *2*, 762−771.

[10] [10a] K. C. Murdock, R. C. Child, P. F. Fabio, R. B. Angier, R. E. Wallace, F. E. Durr, R. V. Citarella, *J. Med. Chem.* **1979**, *22*, 1024−1030. [10b] R. E. Wallace, K. C. Murdock, R. B. Angier, F. E. Durr, *Cancer Res.* **1979**, *39*, 1570−1574.

[11] [11a] C. Garbay-Jaureguiberry, C. Esnault, M. Delepierre, P. Laugaa, S. Laalami, J.-B. Le Pecq, B. P. Roques, *Drugs Exptl. Clin. Res.* **1987**, *13*, 353−357. [11b] C. Garbay-Jaureguiberry, M.-C. Barsi, A. Jacquemin-Sablon, J.-B. Le Pecq, B. P. Roques, *J. Med. Chem.* **1992**, *35*, 72−81.

[12] G. J. Atwell, B. F. Cain, B. C. Baguley, G. J. Finlay, W. A. Denny, *J. Med. Chem.* **1984**, *27*, 1481−1485.

[13] C. Bailly, M. Brana, M. J. Waring, *Eur. J. Biochem.* **1996**, *240*, 195−208.

[14] [14a] R. H. Terbrueggen, J. K. Barton, *Biochemistry* **1995**, *34*, 8227−8234. [14b] D. T. Odom, C. S. Parker, J. K. Barton, *Biochemistry* **1999**, *38*, 5155−5163.

[15] M. Perrée-Fauvet, N. Gresh, *Tetrahedron Lett.* **1995**, *36*, 4227−4230.

[16] [16a] R. F. Pasternack, E. J. Gibbs, J. J. Villafranca, *Biochemistry* **1983**, *22*, 2406−2414. [16b] R. F. Pasternack, E. J. Gibbs, in *Metal DNA Chemistry* (Ed.: T. Tullius), American Chemical Society, Washington, DC, **1989**, pp. 59−73. [16c] R. F. Pasternack, E. J. Gibbs, in *Metal Ions in Biological Systems, Vol. 33* (Eds.: A. Sigel, H. Sigel), Marcel Dekker Inc., New York, **1996**, pp. 367−397. [16d] R. J. Fiel, J. C. Howard, E. H. Mark, N. Datta-Gupta, *Nucleic Acids Res.* **1979**, *6*, 3093−3118.

[17] [17a] D. Praseuth, A. Gaudemer, J. B. Verlhac, I. Kraljic, I. Sissoëff, E. Guillé, *Photochem. Photobiol.* **1986**, *44*, 717−724. [17b] R. W. Byrnes, R. J. Fiel, N. Datta-Gupta, *Chem.-Biol. Interact.* **1988**, *67*, 225−241.

[18] [18a] A. Villanueva, L. Caggiari, G. Jori, C. Milanesi, *J. Photochem. Photobiol., B: Biol.* **1994**, *23*, 49−56. [18b] A. Villanueva, A. Juarranz, V. Diaz, J. Gomez, M. Canete, *Anti-Cancer Drug Des.* **1992**, *7*, 297−303.

[19] N. Gresh, M. Perrée-Fauvet, *J. Comput.-Aided Mol. Des.* **1999**, *13*, 123−137.

[20] P. Konig, R. Giraldo, L. Chapman, D. Rhodes, *Cell* **1996**, *85*, 125−136.

[21] S. Mohammadi, M. Perrée-Fauvet, N. Gresh, K. Hillairet, E. Taillandier, *Biochemistry* **1998**, *37*, 6165−6178.

[22] [22a] A. Tsimanis, V. Bichko, D. Dreilina, J. Meldrais, V. Lozha, R. Kukaine, E. Gren, *Nucleic Acids Res.* **1983**, *11*, 6079−6087. [22b] F. D. Hong, H.-J. S. Huang, H. To, L.-J. S. Young, A. Oro,

R. Bookstein, E. Y.-H. P. Lee, W.-H. Lee, *Proc. Natl. Acad. Sci. U. S. A.* **1989**, *86*, 5502−5506. [22c] M. Dvorak, P. Urbanek, P. Bartunek, V. Paces, J. Vlach, V. Pecenka, L. Arnold, M. Travnicek, J. Riman, *Nucleic Acids Res.* **1989**, *17*, 5651−5664. [22d] S. Smith, D. Baker, L. Jardines, *Biochem. Biophys. Res. Commun.* **1989**, *160*, 1397−1402. [22e] Y. Timsit, D. Moras, *J. Mol. Biol.* **1995**, *251*, 629−647.

[23] [23a] S. Wain-Hobson, P. Sonigo, O. Danos, S. Cole, M. Alizon, *Cell* **1985**, *40*, 9−17. [23b] L. Ratner, W. Haseltine, R. Patarca, K. J. Livak, B. Starcich, S. F. Josephs, E. R. Doran, J. A. Rafalski, E. A. Whitehorn, K. Baumeister, L. Ivanoff, S. R. Petteway Jr, M. L. Pearson, J. A. Lautenberger, T. S. Papas, J. Ghrayeb, N. T. Chang, R. C. Gallo, F. Wong-Staal, *Nature* **1985**, *313*, 277−284.

[24] [24a] J.-B. Le Pecq, M. Le Bret, J. Barbet, B. P. Roques, *Proc. Natl. Acad. Sci. U. S. A.* **1975**, *72*, 2915−2919. [24b] L. P. G. Wakelin, M. Romanos, T. K. Chen, D. Glaubiger, E. S. Canellakis, M. J. Waring, *Biochemistry* **1978**, *17*, 5057−5063. [24c] R. G. Wright, L. P. G. Wakelin, A. Fieldes, R. M. Acheson, M. J. Waring, *Biochemistry* **1980**, *19*, 5825−5836. [24d] H. D. King, W. D. Wilson, E. J. Gabbay, *Biochemistry* **1982**, *21*, 4982−4989. [24e] G. J. Atwell, W. Leupin, S. J. Twigden, W. A. Denny, *J. Am. Chem. Soc.* **1983**, *105*, 2913−2914. [24f] J. B. Hansen, T. Koch, O. Buchardt, P. E. Nielsen, B. Nordén, M. Wirth, *J. Chem. Soc., Chem. Commun.* **1984**, 509−511. [24g] B. Gaugain, J. Markovits, J.-B. Le Pecq, B. P. Roques, *FEBS Lett.* **1984**, *169*, 123−126. [24h] P. Laugâa, J. Markovits, A. Delbarre, J.-B. Le Pecq, B. P. Roques, *Biochemistry* **1985**, *24*, 5567−5575. [24i] M. Wirth, O. Buchardt, T. Koch, P. E. Nielsen, B. Nordén, *J. Am. Chem. Soc.* **1988**, *110*, 932−939. [24j] J. Markovits, C. Garbay-Jaureguiberry, B. P. Roques, J.-B. Le Pecq, *Eur. J. Biochem.* **1989**, *180*, 359−366. [24k] S. C. Zimmerman, C. R. Lamberson, M. Cory, T. A. Fairley, *J. Am. Chem. Soc.* **1989**, *111*, 6805−6809.

[25] [25a] J. W. Lown, S. M. Sondhi, C.-W. Ong, *Biochemistry* **1986**, *25*, 5111−5117. [25b] G. Karagianis, J. A. Reiss, R. Marchesini, M. De Cesare, F. Zunino, D. R. Phillips, *Anti-Cancer Drug Des.* **1996**, *11*, 205−220. [25c] C. Drexler, M. W. Hosseini, G. Pratviel, B. Meunier, *Chem. Commun.* **1998**, 1343−1344. [25d] Y. Ishikawa, A. Yamashita, T. Uno, *Chem. Pharm. Bull.* **2001**, *49*, 287−293.

[26] The binding of MABAP and BABAP to other sequences has been investigated and the results will be presented in a forthcoming paper.

[27] M. Perrée-Fauvet, N. Gresh, *J. Biomol. Struct. Dyn.* **1994**, *11*, 1203−1224.

[28] [28a] A. Pullman, B. Pullman, *Q. Rev. Biophys.* **1981**, *14*, 289−380. [28b] R. Lavery, B. Pullman, *J. Biomol. Struct. Dyn.* **1985**, *5*, 1021−1032.

[29] B. Honig, A. Nicholls, *Science* **1995**, *268*, 1144−1149.

[30] [30a] H. Guo, N. Gresh, B. P. Roques, D. R. Salahub, *J. Phys. Chem. B* **2000**, *104*, 9746−9754. [30b] N. Gresh, J. Sponer, *J. Phys. Chem. B* **1999**, *103*, 11415−11427. [30c] G. Tiraboschi, B. P. Roques, N. Gresh, *J. Comput. Chem.* **1999**, *20*, 1379−1390.

[31] L. A. Carpino, H. Shroff, S. A. Triolo, M. E. Mansour, H. Wenschuh, F. Albericio, *Tetrahedron Lett.* **1993**, *34*, 7829−7832.

[32] L. A. Carpino, G. Y. Han, *J. Am. Chem. Soc.* **1970**, *92*, 5748−5749.

[33] C.-D. Chang, M. Waki, M. Ahmad, J. Meienhofer, E. O. Lundell, J. D. Haug, *Int. J. Pept. Protein Res.* **1980**, *15*, 59−66.

[34] Best yields were obtained recently for the synthesis of new bis and tris-intercalating acridylbis-arginyl-porphyrins by using a Pbf-protected arginine as synthon B.

[35] [35a] M. Wirth, O. Buchardt, T. Koch, P. E. Nielsen, B. Nordén, *J. Am. Chem. Soc.* **1988**, *110*, 932−939. [35b] E. Gimenez-Arnau, S. Missailidis, M. F. G. Stevens, *Anti-Cancer Drug Des.* **1998**, *13*, 125−143 and 431−451.

[36] [36a] W. Keller, *Proc. Natl. Acad. Sci. U. S. A.* **1975**, *72*, 4876−4880. [36b] M. Duguet, C. Bonne, A.-M. de Recondo, *Biochemistry* **1981**, *20*, 3598−3603.

[37] R. Lavery, K. Zakrzewska, H. Sklenar, *Comput. Phys. Commun.* **1995**, *91*, 135−158.

[38] C. R. Cantor, M. M. Warshaw, H. Shapiro, *Biopolymers* **1970**, *9*, 1059−1077.

[39] W. Muller, D. M. Crothers, *J. Mol. Biol.* **1968**, *35*, 251−290.

[40] J. Sambrook, E. F. Fritsch, T. Maniatis, *Molecular Cloning, a Laboratory Manual*, 2nd ed., Cold Spring Harbor Laboratory Press, Plainview, NY, **1989**.

[41] A. Kossanyi, B. Mestre, M. Perrée-Fauvet, *Synth. Commun.* **1999**, *29*, 4341−4346.

Received May 20, 2003

